Fluid flow induces mechanosensitive ATP release, calcium signalling and Cl^- transport in biliary epithelial cells through a PKCζ-dependent pathway

Kangmee Woo[1], Amal K. Dutta[1], Vishal Patel[2], Charles Kresge[1] and Andrew P. Feranchak[1]

[1]*Department of Pediatrics and* [2]*Internal Medicine, University of Texas Southwestern Medical Center, Dallas, TX 75390-9063, USA*

ATP in bile is a potent secretogogue, stimulating cholangiocyte Cl^- and fluid secretion via binding to membrane P2 receptors, though the physiological stimuli involved in biliary ATP release are unknown. The goal of the present studies was to determine the potential role of fluid flow in biliary ATP release and secretion. In both human Mz-Cha-1 biliary cells and normal rat cholangiocyte monolayers, exposure to flow increased relative ATP release which was proportional to the shear stress. In parallel studies, shear was associated with an increase in $[Ca^{2+}]_i$ and membrane Cl^- permeability, which were both dependent on extracellular ATP and P2 receptor stimulation. Flow-stimulated ATP release was dependent on $[Ca^{2+}]_i$, exhibited desensitization with repetitive stimulation, and was regulated by PKCζ. In conclusion, both human and rat biliary cells exhibit flow-stimulated, PKCζ-dependent, ATP release, increases in $[Ca^{2+}]_i$ and Cl^- secretion. The finding that fluid flow can regulate membrane transport suggests that mechanosensitive ATP release may be a key regulator of biliary secretion and an important target to modulate bile flow in the treatment of cholestatic liver diseases.

(Resubmitted 25 February 2008; accepted after revision 31 March 2008; first published online 3 April 2008)
Corresponding author A. Feranchak: UT Southwestern Medical Center, 5323 Harry Hines Boulevard, Dallas, TX 75390-9063, USA. Email: drew.feranchak@utsouthwestern.edu

ATP has emerged as an important signalling molecule regulating hepatobiliary function. Released into bile by both hepatocytes and cholangiocytes, ATP functions as a potent autocrine/paracrine stimulus for cholangiocyte secretion via activation of plasma membrane purinergic (P2) receptors (Feranchak & Fitz, 2002). The concentration of ATP in human bile is within the physiological range for stimulation of P2Y2 and P2X4 (Chari *et al.* 1996), the most abundant P2 receptors in cholangiocytes (Taylor *et al.* 1999; Dranoff *et al.* 2001; Doctor *et al.* 2005). P2 receptor binding results in rapid increases in intracellular calcium concentration and activation of membrane Cl^- channels in both rat and human biliary epithelial models (Roman *et al.* 1999). The resulting increase in transepithelial Cl^- secretion contributes importantly to transport of water and HCO_3^-, resulting in dilution and alkalinization of bile (Fitz, 1996). Modulation of the biliary concentration of ATP therefore may be an important regulator of biliary secretion and bile formation, though the physiological stimulus for cholangiocyte ATP release is unknown.

In other epithelial cells, the most potent stimuli for ATP release are physical or mechanical forces acting at the plasma membrane such as stretch or distention (Knight *et al.* 2002), deformation (Patel *et al.* 2005), pressure (Wang *et al.* 2005), and flow or shear stress (Bodin & Burnstock, 2001). These same physical forces have been associated with secondary messenger generation (Chen *et al.* 2000), ion channel activation (Roman *et al.* 1996; Feranchak *et al.* 1998; Satlin *et al.* 2001), and gene and protein expression (Nakatsuka *et al.* 2006). Thus, ATP release and autocrine/paracrine stimulation of membrane P2 receptors appears to be a key regulatory step linking membrane-directed forces to coordinated cellular responses. For example, ATP release in response to flow/shear force has been shown to regulate vascular bed remodelling, cell differentiation and responses to inflammation in vascular endothelial cells (Dull & Davies, 1991; Bodin & Burnstock, 2001; Farias *et al.* 2005), prostaglandin release in osteoblasts (Genetos *et al.* 2005), and airway surface-fluid volume and composition in respiratory epithelial cells (Tarran *et al.* 2006).

Biliary epithelial cells are also exposed to plasma membrane-directed forces, including membrane tension due to cell swelling (e.g. osmotic gradients, uptake of organic solutes or bile acids (Lira *et al.* 1992; Lazaridis *et al.* 1997)), pressure/distention due to pathological conditions associated with biliary obstruction, and flow/shear forces at the apical membrane due to changes in bile flow. The

This paper has online supplemental material.

 DOI: 10.1113/jphysiol.2008.153015

hormone secretin, for example, increases bile flow from 0.67 to 1.54 ml min^{-1} in humans (Lenzen *et al.* 1997), representing a potential increase in flow-induced force at the apical cholangiocyte membrane. Recently, it has been shown in isolated rat bile duct segments that flow significantly increases $[Ca^{2+}]_i$ (Masyuk *et al.* 2006). Our present studies, in human and rat biliary epithelial models, demonstrate for the first time that the force of flow at the surface of the plasma membrane is a significant and physiological stimulus for ATP release, Ca^{2+} signalling and Cl^- transport. We therefore propose that the mechanical force generated by flow may directly regulate cholangiocyte secretory events and bile formation.

Methods

Cell models

Studies were performed in human Mz-Cha-1 cells and normal rat cholangiocyte (NRC) monolayers. Mz-Cha-1 cells, originally isolated from human adenocarcinoma of the gallbladder (Knuth *et al.* 1985), were passaged at weekly intervals (stock cells were utilized within 1–10 passages) and maintained in culture with HCO_3^--containing CMRL-1066 media (Gibco BRL, Grand Island, NY, USA) supplemented with 10% fetal bovine serum, penicillin (100 IU ml^{-1}) and streptomycin (100 μg ml^{-1}) at 37°C in 5% CO_2. Mz-Cha-1 cells exhibit phenotypic features of differentiated biliary epithelium (Knuth *et al.* 1985; Basavappa *et al.* 1993) and have been utilized as models for biliary ATP release, degradation and signalling (Roman *et al.* 1996, 1999; Wang *et al.* 1997; Feranchak *et al.* 1999, 2004). In preparation for ATP release studies, cells were plated directly onto poly D-lysine (Sigma-Aldrich, St Louis, MO, USA) -treated coverslips on the bottom of the fully assembled perfusion chamber (described below) and grown to confluence. NRC, originally isolated from intrahepatic bile ducts (Vroman & LaRusso, 1996), express phenotypic features of differentiated biliary epithelium including receptors, signalling pathways and ion channels similar to those found in primary cells (Schlenker *et al.* 1997; Salter *et al.* 2000*a*). NRC monolayers were cultured on rat tail collagen slabs as previously described (Schlenker *et al.* 1997; Salter *et al.* 2000*b*) and plated onto collagen-coated (rat collagen, Cell Applications, San Diego, CA, USA) 40 mm glass coverslips (Bioptechs Inc., Butler, PA, USA) 2–5 days prior to study. Polycarbonate spacers were designed to cover the coverslip, exposing only the area corresponding to the flow path when the chamber was assembled (described below), thus preventing cells growing on the area that would be covered by the gasket.

Cilia staining

Antibody staining was performed by incubating the cells with primary antibody to acetylated tubulin (Sigma, 1 : 1000), at 4°C overnight or at room temperature (RT) for 2 h after fixation with 4% paraformaldehyde (4°C for 10 min), antigen retrieval with 1% SDS in 1× PBS for 10 min, and blocking with 10% goat serum, 0.3% bovine serum albumin in 1× PBS for 1 h. The cells were incubated with appropriate secondary antibodies for 1 h at RT in the dark. The slides were mounted with vectashield and coverslipped. The LSM (Zeiss) 510 Meta scanning confocal microscope was utilized for visualization and photography of the images. Imaris 5.0 software (Bitplane Inc., Saint Paul, MN, USA) was utilized for the 3-dimensional reconstruction of the Z-stacks. Results of cilia staining are shown in Supplemental Fig. 1.2.

Perfusion system

Shear was applied to cells in one of several flow chambers to ensure that responses were robust across several model systems. For ATP release measurements from Mz-Cha-1 cells, which are not polarized, a parallel plate flow chamber was designed consisting of an ovoid shape with interior dimensions of 12 mm × 8.2 mm × 1.9 mm and a radius of curvature on the sides of 1.8 mm giving the chamber a rounded diamond shape with curved vertices to promote laminar flow (patent pending); and for NRC, which are polarized monolayers, we utilized a parallel plate chamber (22 mm × 14 mm × 1 mm, Bioptechs Inc. FCS-2) with a 1 mm thick gasket that was compatible with the 40 mm coverslips. A parallel plate chamber (24 mm × 13 mm × 4.1 mm, RC-25F, Warner Instruments, Hamden, CT, USA) was used for Ca^{2+} imaging as well as for whole-cell patch clamp, modified in the latter case by an open top. In each case, flow was applied by a dual syringe pump (Pump 33, Harvard apparatus, Holliston, MA, USA). The equation relating shear stress to volumetric flow rate through the chambers is given by $\tau_w = 6\mu\dot{Q}/a^2b$, where μ is the viscosity of the solution (poise), $\dot{Q}$ is the flow rate (ml s^{-1}), a is the chamber height and b is the chamber width (cm). Two flow protocols were utilized as indicated: (i) a constant flow exposure with incremental increases in the flow rate, or (ii) a multiple-stimulation protocol using a 'start–stop' approach with short flow exposures (shear of 0.32 dyne cm^{-2}) for 15 s and then repeated after a defined interval. The multiple stimulation protocol was used to assess the degree of desensitization, or rate of ATP depletion, which was calculated by measuring the slope of the line generated after plotting the absolute change in arbitrary light units (ALUs) with each flow exposure/maximum absolute ΔALU after 1st flow exposure.

LDH release

Lactate dehydrogenase (LDH) measurements were performed pre- and post-flow exposure using an enzymatic colourimetric cytotoxicity assay (CytoTox 96,

Promega, Madison, WI, USA) as previously described (Spagnou *et al.* 2004). Aliquots of 50 μl were sampled from the bathing solution at baseline and from the efflux solution after the perfusion. Calibration of the assay was performed with cell-free controls and reagents only (no LDH release), LDH standard at a dilution of 1 : 5000 (amount LDH in ~13 000 lysed cells), and values after exposure of cells to lysis solution (maximum LDH release).

ATP detection assay

Cellular ATP release was studied using the luciferin–luciferase (L–L) assay as previously described (Taylor *et al.* 1998; Roman *et al.* 1999; Feranchak *et al.* 2000). In brief, Mz-Cha-1 cells were grown to confluence in the perfusion chamber and prior to study the media was removed, cells were washed with PBS (600 μl $\times$2) and then Optimem (Gibco) was added to fill the chamber. For experiments of NRC, the spacers were removed and the coverslips were washed with PBS (600 μl $\times$2), and placed in the perfusion chamber. Once the individual chambers were assembled, the in- and outflow ports of the syringe pump (see below) were connected via silastic tubing (Dow Corning, Midland, MI, USA). The chamber was then perfused with Optimem at a low flow rate (shear = 0.08 dyne cm^{-2}) to replace all the Optimem in the chamber and allowed to equilibrate for 10 min. Defined shear was then applied and 60 μl aliquots from the outflow port were collected every 30 s and added to 4 μl of L–L reagent (Fl-ATP Assay Mix, Sigma: reconstituted according to manufacturer's directions and used at a final dilution of 1 : 15) and luminescence immediately measured over a 15 s photon interval in a modified Turner TD 20/20 Luminometer and reported as arbitrary light units (ALUs). At the start of the each experiment a low flow rate was applied (shear = 0.08 dyne cm^{-2}), to provide an aliquot for LDH measurement, and five sequential luminescence measurements for 'basal' levels (it should be noted that once the parallel-plate chamber is assembled, measurements in the absence of any flow exposure are not possible); no increase in luminescence was observed at this low shear. Shear was then increased as indicated. Separate studies were performed to measure any potential ATP release during static or no flow conditions. For these studies, Mz-Cha-1 cells were grown to confluency (in the same perfusion chambers used for the flow studies), washed with Optimem, bathed with Optimem + L–L (1 : 15 dilution), placed in the luminometer, and, after a 10 min equilibration period, 'real-time' luminescence measurements were obtained every 30 s. All luminescence values are reported as relative change from basal luminescence to control for any potential difference in luciferase activity between batches of reagent. Standard calibration curves were performed with known amounts of ATP added to the L–L + Optimem reagent during cell-free conditions (Supplemental Fig. 1.1A). Both the real-time and sampling ATP assays were performed at room temperature, as luciferase activity decreases at 37°C as shown in Supplemental Fig. 1.1C and previously reported (Ueda *et al.* 1994).

Ca^{2+} imaging

Cells were cultured for 48 h on 15 mm glass coverslips and then loaded with 2.5 μg ml^{-1} of fura-2 AM (TEF Laboratories, Austin, TX, USA) in isotonic extracellular buffer containing (mM): 140 NaCl, 4 KCl, 2$CaCl_2$, 1 $MgCl_2$, 1 KH_2PO_4, 5 glucose, 10 Hepes (pH 7.4) supplemented with 0.01% pluronic F127 for 30 min at 22°C. In selected studies, Ca^{2+} was removed from the bath and perfusing solutions by EGTA (2 mM). The coverslip was placed in the perfusion chamber on the stage of an inverted fluorescent microscope (Nikon TE2000) and the inflow and outflow ports were attached to the syringe pump. Changes of $[Ca^{2+}]_i$ were measured at excitation wavelength of 340 nm for calcium-bound fura-2 AM and 380 nm for calcium-free fura-2 AM, emission wavelength of 510 nm. After subtracting background fluorescence, $[Ca^{2+}]_i$ was calculated according to Grynkiewicz equation (Simpson, 1999):

$$[Ca^{2+}]_i(\text{nM}) = K_d \times [(R - R_{\min})/(R_{\max} - R)] \times \text{Sfb}$$

(K_d at 22°C = 145; Sfb, ratio of baseline fluorescence (380 nm) under Ca^{2+}-free and -bound conditions). Experiments were performed at room temperature (for comparison with ATP release studies) and at 37°C.

Measurement of flow-stimulated currents

Membrane currents were measured using whole-cell patch clamp techniques. Cells on a coverslip were mounted in the chamber and whole-cell currents measured during basal and perfused conditions with a standard extracellular solution containing (mM): 140 NaCl, 4 KCl, 1 $CaCl_2$, 2 $MgCl_2$, 1 KH_2PO_4, 10 glucose and 10 Hepes/NaOH (pH ~7.40). The standard intracellular (pipette) solution for whole-cell recordings contained (mM): 130 KCl, 10 NaCl, 2 $MgCl_2$, 10 Hepes/KOH, 0.5 $CaCl_2$ and 1 EGTA (pH 7.3), corresponding to a free $[Ca^{2+}]$ of ~100 nM (Chang *et al.* 1988; Feranchak *et al.* 2001). For selected studies, extracellular monovalent cations were replaced with NMDG and intracellular monovalent cations were replaced with TEA. Patch pipettes were pulled from Corning 7052 glass and had a resistance of 3–10 MΩ. Recordings were made with an Axopatch ID amplifier (Axon Instruments, Foster City, CA, USA), digitized (1 kHz) and analysed using pCLAMP version 10

(Axon Instruments, Burlingame, CA, USA) as previously described (Fitz & Sostman, 1994; Feranchak *et al.* 2001). Two voltage protocols were utilized: (1) holding potential −40 mV, with 200 ms steps to 0 mV and −80 mV at 10 s intervals, and (2) holding potential −40 mV, with 400 ms steps from −100 mV to +100 mV in 20 mV increments. Current–voltage (I–V) relations were generated from the 'step' protocol. Pipette voltages (V_p) are referred to the bath. Results are compared with control studies measured on the same day to minimize any effects of day-to-day variability. While mean cell capacitance was 20.4 ± 1.1 pF, results are reported as current density (pA pF^{-1}) to normalize for differences in cell size (Feranchak *et al.* 2001).

Reagents

Thapsigargin was obtained from Calbiochem/EMD Biosciences (La Jolla, CA, USA), calphostin C from MP Biomedicals (Solon, OH, USA), and myristoylated and scrambled protein kinase C (PKC) ζ pseudosubstrate from Quality Controlled Biochemicals (Hopkinton, MA, USA). All other reagents were obtained from Sigma-Aldrich. None of the PKC inhibitors (chelerythrine, calphostin C, myristoylated PKCζ pseudosubstrate and phorbol 12-myristate 13-acetate (PMA)) affected the L–L reaction as measured during cell-free conditions.

Statistics

Results are presented as the mean ± standard error of the mean (S.E.M.), with n representing the number of culture plates or repetitions for each assay as indicated. Statistical analysis included Fisher's paired and unpaired t test and ANOVA for multiple comparisons to assess statistical significance as indicated, and P values < 0.05 were considered to be statistically significant.

Results

Increasing flow rates stimulate ATP release from human and rat biliary epithelial cells

Confluent Mz-Cha-1 cells released a small amount of ATP during static (no flow) conditions as detected by arbitrary light units (ALUs) (Fig. 1*A* inset). Measured luminescence, which decreased over time, was specific for extracellular ATP as the addition of the ATP scavenger apyrase (2 Units ml^{-1}) rapidly abolished luminescence ($n = 6$). To determine whether Mz-Cha-1 cells release ATP in response to flow, the amount of ATP in the perfusate was measured in response to defined shear stress. After the parallel plate chamber with confluent cells was assembled, a low flow was applied (shear = 0.08 dyne cm^{-2}) and ATP release measured (Fig. 1*A*). During this low flow exposure no increase in luminescence was observed; in fact, a steady decline in luminescence was noted which paralleled that observed in cells under static conditions, and hence these initial measurements were considered basal levels. Increasing flow to generate a shear of 0.16 dyne cm^{-2}, resulted in a rapid increase in ATP release within seconds, with a maximum relative increase of 1.67 ± 0.21 ALUs observed at 1 min compared to a relative change of 0.83 ± 0.01 ALUs in control cells without flow at the same time point ($n = 6$; $P < 0.01$; Fig. 1*A*). Increasing the shear to 0.64 dyne cm^{-2} resulted in a further increase in ATP release, with a relative increase of 3.22 ± 0.42 ALUs compared to 0.71 ± 0.01 ALUs in control (no flow) at the same time point ($n = 6$, $P < 0.01$). In separate studies, Mz-Cha-1 cells were exposed to shear of 0.16, 0.32, 0.48 and 0.64 dyne cm^{-2} and ATP release measured. Flow-stimulated ATP release was observed within seconds of the onset of flow and the magnitude of the release was proportional to the shear force applied (Fig. 1*C*).

To determine if similar shear-stimulated ATP release occurs in intact biliary epithelium, confluent NRC monolayers were exposed to shear under identical experimental conditions. Increasing shear from 0.08 (basal) to 0.16 dyne cm^{-2} resulted in a rapid relative increase in ATP release of 2.18 ± 0.11 ALUs observed at 1 min compared to a relative change of 0.92 ± 0.03 ALUs in control cells without flow (inset) at the same time point ($n = 6$; $P < 0.01$; Fig. 1*B*). Increasing the shear to 0.64 dyne cm^{-2} resulted in a further increase in ATP release, with a relative increase of 3.29 ± 0.26 ALUs compared to a change of 0.84 0.04 ALUs in control cells (no flow) at the same time point ($n = 6$, $P < 0.01$). In separate studies, NRC monolayers were exposed to shear of 0.17, 0.35, 0.53 and 0.71 dyne cm^{-2} and ATP release measured. Flow-stimulated ATP release was observed within seconds of the onset of flow and proportional to shear stress up to 0.53 dyne cm^{-2} (shear above this level was not associated with any further significant increase in ATP release, Fig. 1*C*). While both Mz-Cha-1 and NRC demonstrated flow-stimulated ATP release, the relative magnitude of ATP release in NRC was greater than Mz-Cha-1 for a similarly applied shear stress (Fig. 1*C*). The relative increase in flow-stimulated ATP release, measured as ALUs, can be converted to absolute ATP concentrations by comparison to standard curves generated by cell-free studies with known amounts of ATP (Supplemental Fig. 1.1A). Thus, the maximum relative ATP release measured at 0.64 dyne cm^{-2} corresponded to an actual ATP concentration of ∼94 ± 18 nM for Mz-Cha-1 and ∼110 ± 24 nM for NRC (Fig. 1*D*). To exclude cell lysis as a source of extracellular ATP, LDH measurements were performed on samples taken during the initial low flow exposure (basal reading) and from the efflux port at the end of the flow exposure (shown in Supplemental Tables 1 and 2).

No significant difference in LDH release was observed pre- and post-perfusion.

Flow-stimulated ATP release requires intracellular Ca^{2+}

It has previously been shown that swelling-induced ATP release is dependent on $[Ca^{2+}]_i$ in rat hepatoma cells (Feranchak *et al.* 2000). To determine if mechanosensitive ATP release in response to flow/shear is also dependent on intracellular $[Ca^{2+}]_i$, studies were performed in Mz-Cha-1 cells with or without prior treatment with BAPTA-AM (50 μM) to chelate intracellular $[Ca^{2+}]_i$. In control cells, an increase in shear from 0.08 to 0.32 dyne cm^{-2} was associated with a relative increase of ATP release of 1.65 ± 0.12 ALUs, respectively. After

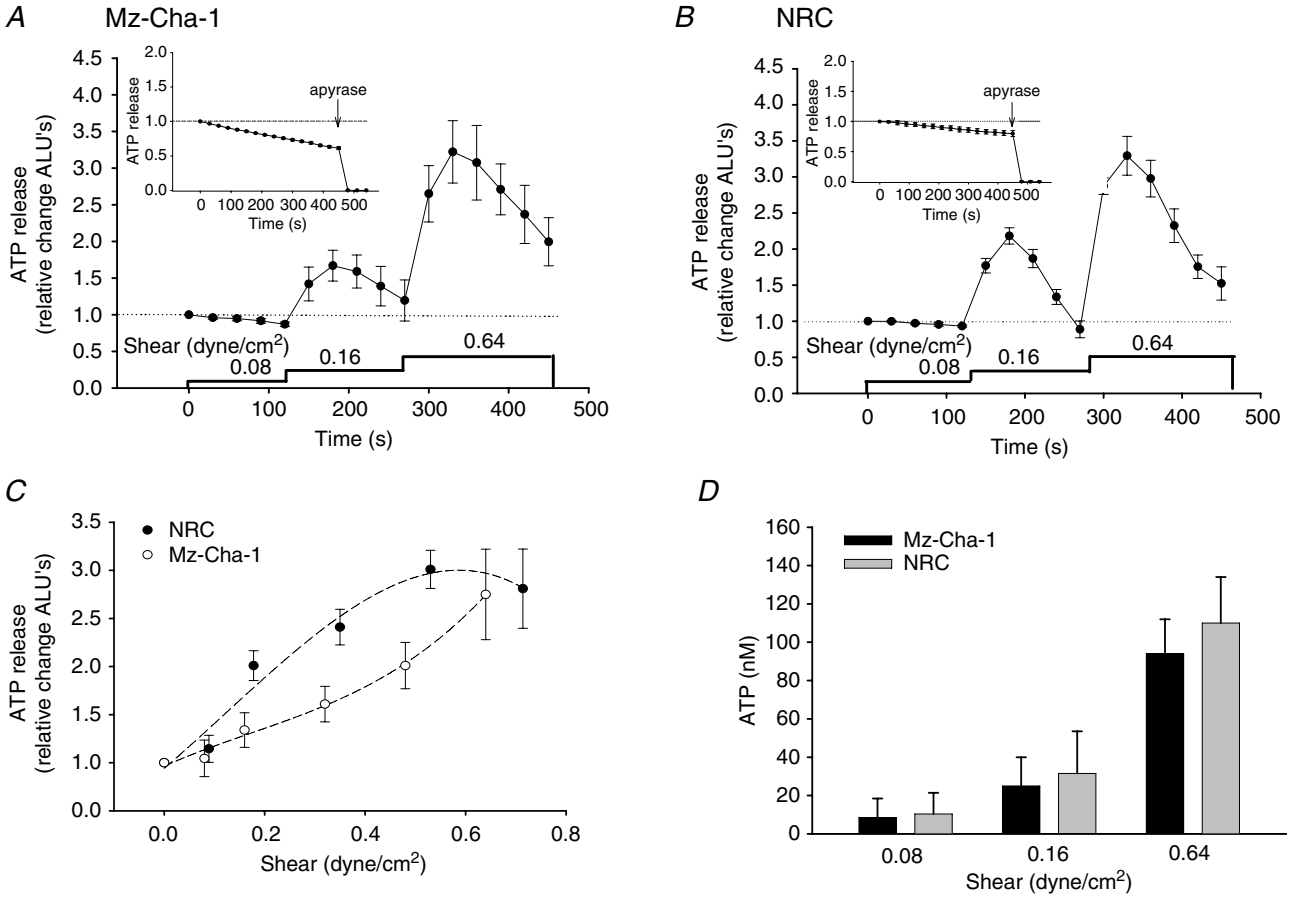

Figure 1. Mechanical flow stimulates ATP release from human and rat biliary epithelial cells
A, flow-stimulated ATP release from human Mz-Cha-1 cells. During static (no flow) conditions a gradual decline in luminescence occurs as ATP released during the initial washing procedure is hydrolysed, while addition of apyrase (2 Units ml^{-1}) completely hydrolyses ATP and abolishes luminescence (inset) ($n = 6$). In separate studies, confluent Mz-Cha-1 cells were perfused with Optimem and 60 μl aliquots were taken from the efflux every 30 s, added to standard L–L reagent, and immediately placed in the luminometer for luminescence measurement. No increase in ATP release was observed during exposure to low flow (shear 0.08 dyne cm^{-2}). However, ATP release increased within seconds of increasing shear to 0.16 dyne cm^{-2}, and increased further upon a step-increase in shear to 0.64 dyne cm^{-2} ($n = 6$). Bars along bottom indicate length of flow/shear exposure. *B*, flow-stimulated ATP release from normal rat cholangiocyte (NRC) monolayers. Experimental protocol same as described in *A*. During static (no flow) conditions a gradual decline in luminescence occurs, while addition of apyrase (2 Units ml^{-1}) completely hydrolyses ATP and abolishes luminescence (inset) ($n = 6$). Exposure to increasing shear (0.16 and 0.64 dyne cm^{-2}) results in significant increases in the magnitude of ATP release ($n = 6$). *C*, in separate studies, defined shear stresses were applied to either Mz-Cha-1 (○) or NRC monolayers (●) and ATP release recorded. Values represent the maximum luminescence within 1 min of flow/shear exposure ($n = 4$–6 for each). Points fitted by best-fit 2nd order regression analysis. *D*, cumulative data demonstrating actual extracellular ATP concentration detected in media under flow-stimulated (shear of 0.08, 0.16 and 0.64 dyne cm^{-2}) conditions, based on ATP standard curves (Supplemental Fig. 1.1A) for Mz-Cha-1 cells (black bars) or NRC monolayers (grey bars). Values represent maximum ATP concentration within 1 min of flow/shear exposure ($n = 6$ each).

exposure to BAPTA-AM, the response to shear decreased to only 0.91 ± 0.04 ALUs ($n = 6$ for each, $P < 0.05$, Fig. 2). Addition of apyrase (2 Units ml^{-1}) to the perfusing solution abolished luminescence in both control and BAPTA-treated cells (Fig. 2*A* and *B*). In the absence of flow, exposure to ionomycin (2 μM), to acutely and maximally elevate $[Ca^{2+}]_i$, resulted in a relative increase of only 1.10 ± 0.08 ALUs, which was comparable in magnitude to flow-stimulated ATP release at low shear (0.16 dyne cm^{-2}), but significantly less than that observed at shear ≥ 0.32 dyne cm^{-2} (1.61 ± 0.18 ALUs at 0.32 dyne cm^{-2}, $n = 5$, $P < 0.05$; Fig. 2*B*). Together these studies demonstrate that Ca^{2+} is necessary for flow-stimulated ATP release; however, an acute elevation in $[Ca^{2+}]_i$ alone is only a minimal stimulus for ATP release.

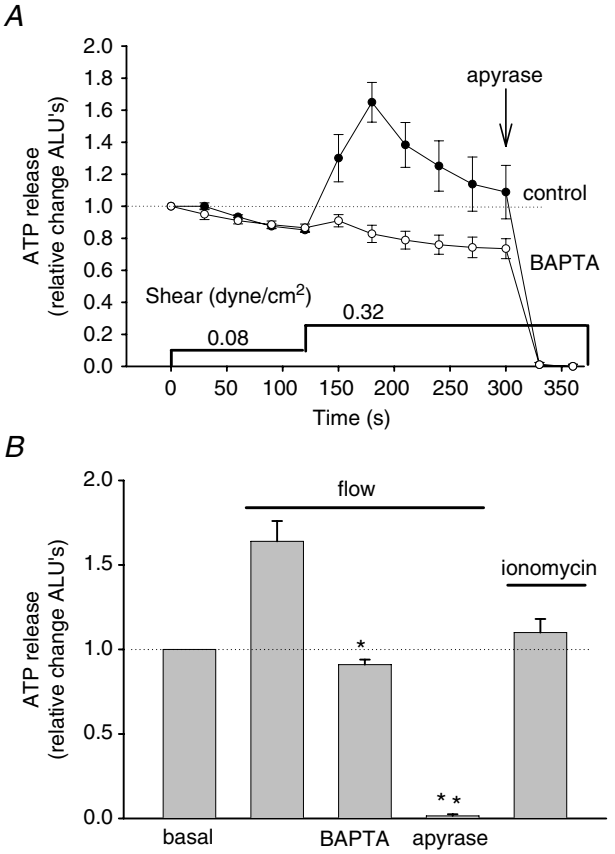

Figure 2. Flow-stimulated ATP release is dependent on intracellular Ca^{2+}
A, in control Mz-Cha-1 cells, increasing shear from 0.08 to 0.32 dyne cm^{-2} resulted in an increase in ATP release (●). Pre-incubation of cells with BAPTA-AM (50 μM) significantly decreased flow-stimulated ATP release (○). Addition of apyrase (2 Units ml^{-1}) to the perfusate rapidly abolished luminescence in both control and BAPTA-AM-treated cells. Values represent mean ± S.E.M. ($n = 5$ each). *B*, cumulative data demonstrating relative change in ATP release with flow (shear 0.32 dyne cm^{-2}) or ionomycin. *BAPTA-AM significantly inhibited flow-stimulated (shear 0.32 dyne cm^{-2}) ATP release ($P < 0.05$). **Apyrase (2 Units ml^{-1}) abolished flow-stimulated luminescence ($P < 0.01$). In the absence of flow, acute elevation of $[Ca^{2+}]_i$ by ionomycin (2 μM) resulted in only a small increase in ATP release. Values represent maximum relative increase in ATP release from basal levels within 1 min of flow or ionomycin exposure ($n = 5$ for each).

Flow stimulates an increase in $[Ca^{2+}]_i$

Recently it has been shown in isolated rat bile duct segments that flow causes an increase in $[Ca^{2+}]_i$ (Masyuk *et al.* 2006). To determine if flow results in similar effects in human Mz-Cha-1 cells and NRC monolayers, cells were loaded with fura-2 and fluorescence measured under basal and flow-stimulated conditions. In Mz-Cha-1 cells, exposure to shear of 0.09 dyne cm^{-2} rapidly increased $[Ca^{2+}]_i$ by an average of 0.012 ± 0.008 relative fluorescence units s^{-1}, reaching a maximum concentration of 279 ± 68 nM within 59.2 ± 13.3 s ($n = 7$, $P < 0.01$ *versus* control, Fig. 3*A* and *D*). Confluent NRC monolayers also demonstrated a significant increase in $[Ca^{2+}]_i$ to 351 ± 167 nM in response to shear of 0.09 dyne cm^{-2} with similar kinetics to Mz-Cha-1 cells ($n = 4$, $P < 0.05$ *versus* control, data not shown). Additional individual studies were performed in Mz-Cha-1 cells with shear of 0.01, 0.02, 0.04, 0.09 and 0.24 dyne cm^{-2}. While shear of 0.01 and 0.02 dyne cm^{-2} resulted in small increases in $[Ca^{2+}]_i$ to 49 ± 16 nM ($n = 4$) and 44 ± 7 nM ($n = 7$), respectively, a threshold appeared to be reached at 0.09 dyne cm^{-2} with a significant increase in $[Ca^{2+}]_i$ to 279 ± 68 nM ($n = 7$, $P < 0.01$, Fig. 3*B*). Exposure to shear of 0.24 dyne cm^{-2} increased $[Ca^{2+}]_i$ to 298 ± 45 ($n = 4$, $P < 0.05$ *versus* control); however, this was not statistically greater than the increase observed with a shear of 0.09 dyne cm^{-2} (Fig. 3*B*). At a shear of 0.09 dyne cm^{-2} studies performed at 37°C resulted in a significant increase in $[Ca^{2+}]_i$ to 470 ± 88 nM ($n = 7$) compared to an increase to 279 ± 68 nM ($n = 7$) in control cells at 23°C (Fig. 3*B* inset). However, there was no difference between the magnitude of flow-stimulated $[Ca^{2+}]_i$ at 37°C *versus* 23°C at lower shear (Fig. 3*B* inset). These findings in human and rat biliary epithelial models are similar to those observed in isolated rat bile duct segments (Masyuk *et al.* 2006) and demonstrate that flow/shear is a significant stimulus modulating $[Ca^{2+}]_i$.

Both extracellular and intracellular Ca^{2+} contributes to the flow-stimulated increase in $[Ca^{2+}]_i$

To evaluate the dependence of flow-stimulated $[Ca^{2+}]_i$ on intra- *versus* extra-cellular Ca^{2+} sources, imaging studies in response to flow (shear = 0.09 dyne cm^{-2}) were performed on fura-2-loaded cells with the selective removal of Ca^{2+} from the buffer and perfusing solutions (EGTA, 2 mM) or after depletion of intracellular stores by thapsigargin. Removal of extracellular

Ca^{2+} from the bath and perfusate had little effect on the rate of rise (0.012 ± 0.006 relative fluorescence units s^{-1}), time to peak fluorescence (50.1 ± 16.2 s), and magnitude of peak fluorescence (271 ± 60 nM, $n = 7$, $P =$ n.s. *versus* 279 ± 68 nM in control, Fig. 3*C* and *D*); however, pre-incubation with thapsigargin (500 nM for 30 min) slowed the rate of rise of fura-2 fluorescence to 0.0061 ± 0.003 relative fluorescence

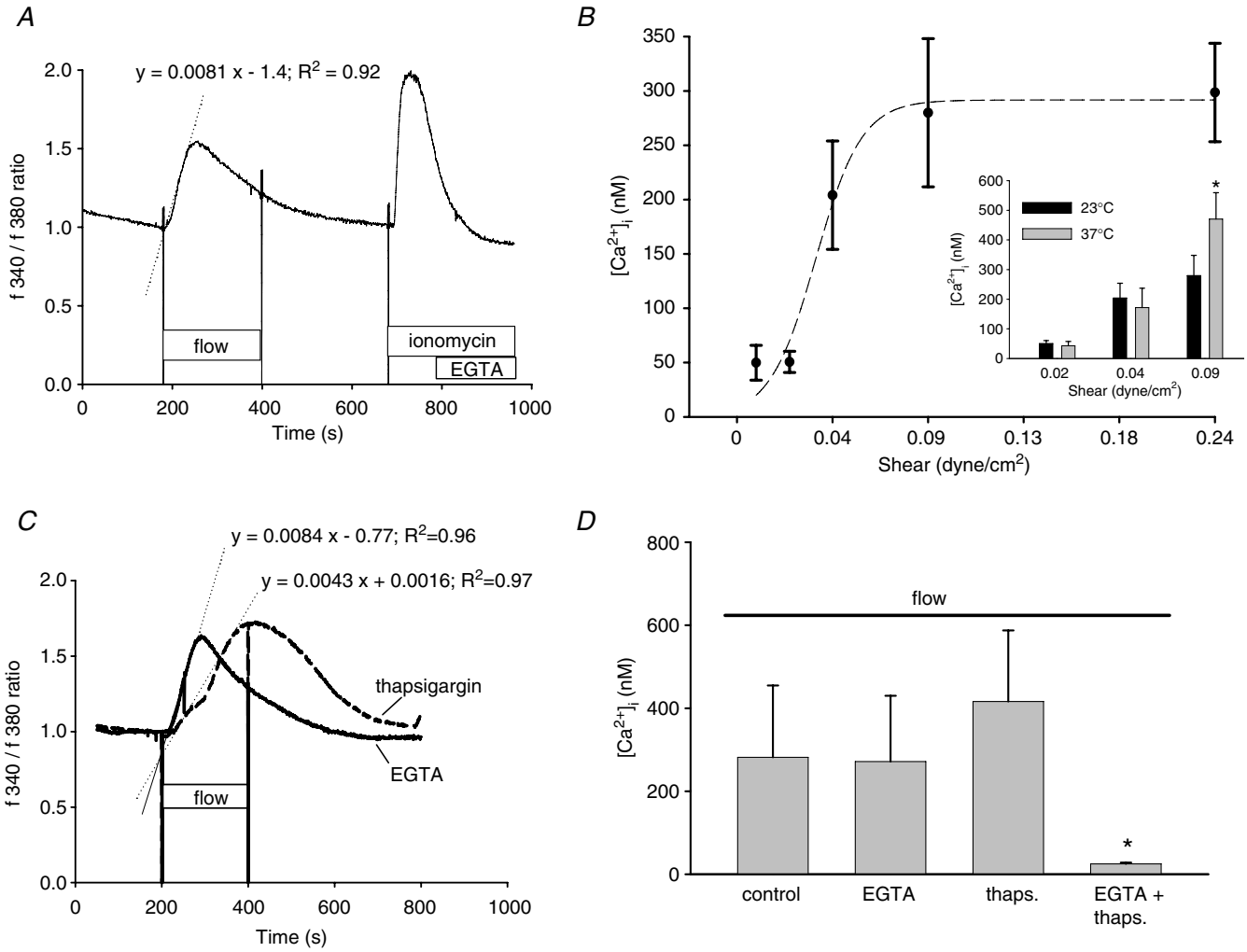

Figure 3. Flow stimulates an increase of $[Ca^{2+}]_i$

Mz-ChA-1 cells grown on a coverglass were loaded with fura-2 AM, washed with PBS and exposed to defined flow rates of isotonic buffer (see Methods). Values represent increase in the ratio of fluorescence at 340 and at 380 nm. *A*, in this representative study, fura-2 fluorescence increased within seconds of flow exposure (shear of 0.09 dyne cm^{-2}, indicated by the bar) at a rate of 0.008 relative fluorescence units s^{-1} (indicated by the dotted line), reached a maximal value at 30 s, and then decreased to basal levels. Maximal and minimal $[Ca^{2+}]_i$ was obtained by exposure to ionomycin (2 μM) and EGTA (10 mM), respectively. *B*, in separate studies, cells were perfused at different flow rates (shear of 0.09, 0.02, 0.04, 0.09 and 0.24 dyne cm^{-2}) and maximal fura-2 fluorescence recorded. Little increase in fura-2 fluorescence was observed at shear stresses of < 0.04 dyne cm^{-2} while the maximum Ca^{2+} signal was observed at shear of 0.09 dyne cm^{-2} ($n = 4$–7 for each). *B* (inset), increasing the temperature to 37°C (grey bars) resulted in a significant increase in $[Ca^{2+}]_i$ at a shear of 0.09 compared with 23°C (black bars) ($n = 7$ for each, $^*P < 0.01$). There was no difference in the magnitude of $[Ca^{2+}]_i$ between 23°C and 37°C at a shear of 0.02 or 0.04 dyne cm^{-2} ($n = 4$ each, $P =$ n.s.) *C*, both extracellular and intracellular Ca^{2+} contribute to the increase in flow-induced $[Ca^{2+}]_i$. In separate studies, Mz-ChA-1 cells were incubated with either thapsigargin (500 nM for 30 min) or Ca^{2+}-free buffer (EGTA, 2 mM, for 5 min), loaded with fura-2 AM and exposed to flow (shear 0.09 dyne cm^{-2}). Removal of extracellular Ca^{2+} (EGTA) from the perfusate had no effect on flow-stimulated fura-2 fluorescence, demonstrating a rate of rise of 0.008 fluorescence units s^{-1} and a maximal increase at 58 s. Removal of intracellular Ca^{2+} stores (thapsigargin) decreased the rate of rise to 0.004 fluorescence units s^{-1} and delayed the time to peak fluorescence ($n = 5$, $P < 0.05$) (dashed line). *D*, cumulative data. The magnitude of the flow-stimulated (shear of 0.09 dyne cm^{-2}) increase in $[Ca^{2+}]_i$ was unaffected by individual removal of extracellular (EGTA, $n = 7$) or depletion of intracellular (thapsigargin, $n = 5$) Ca^{2+}, but significantly inhibited when both were simultaneously depleted ($n = 3$, $^*P < 0.05$). Values represent the maximal $[Ca^{2+}]_i$ in nM.

units s^{-1} (a 50% decrease in rate) and prolonged the time to peak fluorescence (104.4 ± 27.5 s, $P < 0.05$), though the magnitude of peak fluorescence was not different from controls (416 ± 70 nM, $n = 5$, $P =$ n.s. *versus* 279 ± 68 nM in control, Fig. 3*C* and *D*). As would be expected, simultaneous removal of both extracellular Ca^{2+} and depletion of intracellular stores completely abolished the flow-stimulated increase in $[Ca^{2+}]_i$ (24 ± 2 nM, $n = 3$, $P < 0.05$ *versus* control, Fig. 3*D*). The finding that removal of extracellular Ca^{2+} had no effect on the onset, rate of rise or magnitude of flow-stimulated fura-2 fluorescence suggests that the observed increase in $[Ca^{2+}]_i$ is primarily through release from an intracellular Ca^{2+} pool. However, the finding that depletion of intracellular Ca^{2+} stores slowed the rate of rise, but did not affect the magnitude, of the calcium signal suggests that extracellular Ca^{2+} is capable of contributing to the flow-stimulated response. Thus, flow-stimulated Ca^{2+} signalling in this biliary model is complex with at least two components involved.

Flow-stimulated Ca^{2+} signalling is dependent on extracellular ATP and P2 receptor stimulation

To determine if flow-stimulated ATP release and flow-stimulated increases in $[Ca^{2+}]_i$ are linked, cells were loaded with fura-2 and exposed to flow, to generate shear of 0.09 dyne cm^{-2}, in the presence or absence of apyrase which rapidly hydrolyses ATP. The flow-stimulated increase in $[Ca^{2+}]_i$ to 345 ± 23 nM observed in control cells ($n = 8$) was significantly inhibited in the presence of apyrase (5 U ml^{-1}) to 63 ± 18 nM ($n = 4$, $P < 0.05$, Fig. 4*A*–*C*). The effects of apyrase on flow-stimulated fura-2 fluorescence were concentration dependent with an apparent K_i of $\sim$2 U ml^{-1} (Fig. 4*C*). Additional studies were performed in the presence or absence of P2 receptor antagonists. In the presence of the P2Y inhibitor, suramin (100 μM), shear-stimulated (0.09 dyne cm^{-2}) increases in $[Ca^{2+}]_i$ were significantly inhibited (47 ± 11 nM, $n = 3$) compared to control (384 ± 157 nM, $n = 6$, $P < 0.01$, Fig. 4*D* and *F*). In contrast, the P2X receptor antagonist, Brilliant Blue G (10 μM), had little effect on flow-stimulated $[Ca^{2+}]_i$ (330 ± 75 nM, $n = 4$, $P =$ n.s. *versus* control, Fig. 4*E* and *F*). Together these results demonstrate that flow-stimulated increases in $[Ca^{2+}]_i$ are dependent on extracellular ATP and P2Y receptor stimulation.

Repetitive flow stimulation results in a depletion of a readily releasable pool of cellular ATP

In many secretory cells the rate of exocytosis decreases significantly upon repeated stimulation due to depletion of a readily releasable pool (RRP) of secretory vesicles (Oheim *et al.* 1999). Additionally, it has previously been shown in Mz-Cha-1 cells that cell swelling-associated ATP release is dependent on exocytosis of a readily releasable ATP pool (Gatof *et al.* 2004). Thus, we adopted a multiple-stimulation protocol, with repetitive short flow exposures, as a functional assay of the ATP RRP in Mz-Cha-1 cells. When cells were exposed to repetitive flow exposures (shear of 0.32 dyne cm^{-2} for 15 s, repeated every 1 min) the magnitude of ATP release decreased with each subsequent exposure (Fig. 5*A*) consistent with depletion of a finite, RRP of ATP. The time constant ($t_{1/2}$ depletion) for emptying the RRP of ATP with this repetitive flow stimulus was $\sim$1.7 min (Fig. 5*B*), which is consistent with the time needed for replenishment of secretory vesicles in chromaffin cells after a depolarizing stimulus (Steyer *et al.* 1997). Additionally, with a repetitive flow/shear stimulus of 0.32 dyne cm^{-2} for 15 s the rate of depletion of the ATP RRP was accelerated as the time between stimuli was shortened (Fig. 5*C*). At an interval of 5 min between flow exposures, the magnitude of maximal ATP release was similar with each stimulus with a rate of depletion of only 0.004 ALUs per perfusion, which reflects an adequate time for refilling the pool of releasable ATP; however, when the interval between flow stimuli was shortened to 40 s the rate of depletion increased to 0.49 ALUs per perfusion, an $\sim$100-fold increase in the depletion rate ($P < 0.01$, Fig. 5*C*). Together these studies demonstrate that a finite, depletable ATP pool exists and provide a functional correlate of the RRP of ATP in biliary cells.

Flow-stimulated ATP release is dependent on PKCζ

In Mz-Cha-1 cells, *swelling-induced* ATP release is regulated in part by PKC which translocates to the membrane within minutes of hypotonic exposure (Roman *et al.* 1998) and increases the amount of ATP in a RRP (Gatof *et al.* 2004). The specific PKC isoform(s) involved in mechanosensitive ATP release, however, have not been determined. To determine if PKC plays a similar regulatory role in flow-stimulated ATP release and, if so, to characterize the particular isoform class involved, the effects of a panel of isoform-selective PKC inhibitors on the magnitude and rate of depletion of flow-stimulated ATP release were determined. In the presence of chelerythrine (1 μM), which inhibits substrate binding to the C4 catalytic domain of all PKC isoforms (Herbert, 1990), maximal flow-stimulated ATP release was reduced by 64.1 ± 2.3% compared to control cells ($n = 6$ each, $P < 0.05$, Fig. 6*A*). Calphostin C, which inhibits the regulatory domain of conventional and novel PKC isoforms, failed to alter the magnitude of flow-stimulated ATP release (decrease of 5.0 ± 2.4%, $n = 5$, $P =$ n.s., Fig. 6*A*); and neither 12–18 h incubation with PMA (1 μM), which interacts with the C1 domain of conventional PKC isoforms to decrease PKC activity, or acute exposure (1 μM

for 5 min) to increase PKC activity altered flow-stimulated ATP release (decrease of $7.0 \pm 4.0\%$, $n = 8$; and increase of $8.0 \pm 6.9\%$, $n = 10$, respectively, $P =$ n.s.). The lack of effect by PMA or calphostin C on ATP release suggested the potential involvement of an atypical PKC isoform. To test this more directly, studies were performed utilizing a specific cell-permeable inhibitor of PKCζ, myristoylated PKCζ pseudosubstrate (Sun *et al.* 2005), and compared to control cells incubated with a scrambled myristoylated PKCζ peptide (10 μM for 10–15 min for each). Compared with control cells, cells incubated with the PKCζ pseudosubstrate demonstrated a $74.6 \pm 3.7\%$

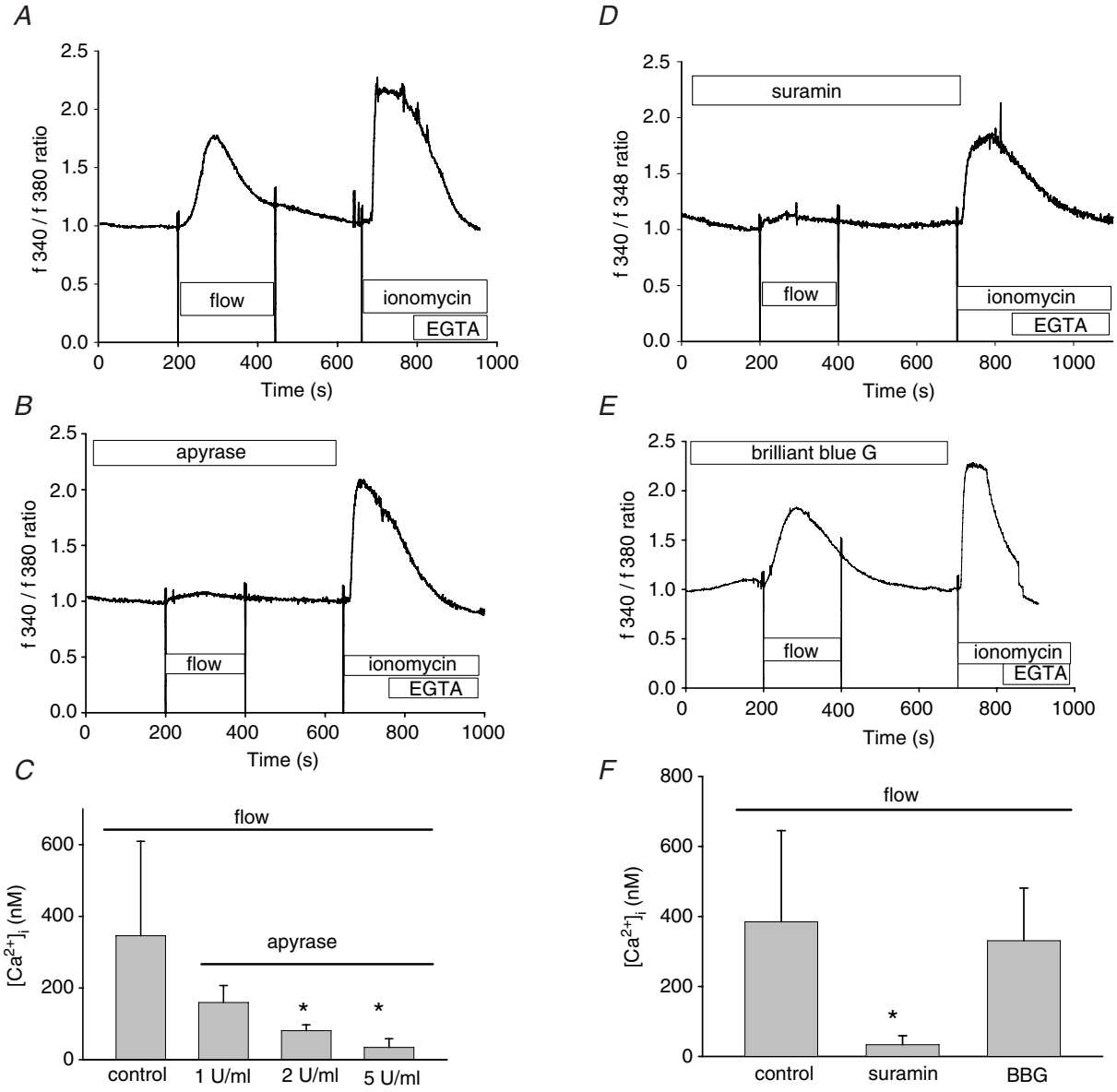

Figure 4. Flow-induced increases in $[Ca^{2+}]_i$ are dependent on extracellular ATP and purinergic receptor stimulation

Fura-2-loaded Mz-Cha-1 cells were exposed to flow (shear of 0.09 dyne cm^{-2}), as indicated by the bar. *A*, representative control study demonstrating an increase in flow-induced $[Ca^{2+}]_i$. *B*, in the presence of apyrase (5 Units ml^{-1}) flow-stimulated fura-2 fluorescence was inhibited. *C*, inhibition of flow-stimulated fura-2 fluorescence by apyrase was concentration dependent with an apparent K_i of $\sim$2 Units ml^{-1}. Values represent maximum absolute $[Ca^{2+}]_i$ in nM ($n = 4$–8 for each). *D*, in the presence of the P2Y receptor antagonist suramin (100 μM) no increase in fura-2 fluorescence in response to flow was observed. *E*, the P2X receptor antagonist, Brilliant Blue G (10 μM), had little effect on flow-stimulated fura-2 fluorescence. *F*, cumulative data demonstrating the effects of P2 receptor antagonists on flow-stimulated $[Ca^{2+}]_i$. Values represent the maximal flow-stimulated increase in $[Ca^{2+}]_i$ in nM ($n = 3$–6 each). *Suramin significantly inhibited flow-stimulated fura-2 fluorescence ($P < 0.01$).

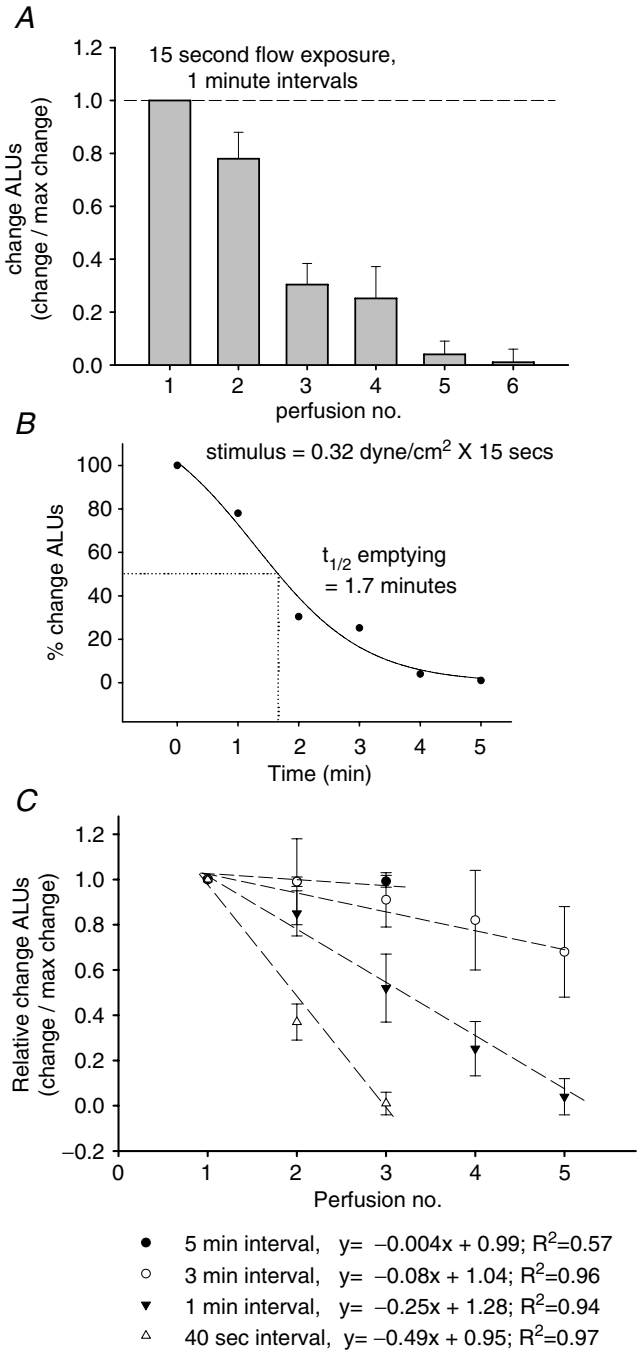

Figure 5. Flow-stimulated ATP release demonstrates desensitization with repetitive flow exposures
Confluent Mz-Cha-1 cells were placed in the flow chamber within a luminometer and ATP release in response to the multiple-stimulation protocol (see Methods) measured using the real-time L–L assay. *A*, in response to repetitive flow exposures (shear of 0.32 dyne cm^{-2} for 15 s) every 1 min the magnitude of ATP release decreased with each successive exposure. Values represent the relative change in luminescence/maximal change in luminescence with the 1st perfusion ($n = 8$ for each). *B*, the available, or readily releasable pool (RRP), of ATP was depleted with a time constant ($t_{1/2}$ emptying) of ~1.7 min in response to repetitive shear exposures of 0.32 dyne cm^{-2} for 15 s every 1 min (points are average of 8 trials fitted with sigmoidal regression). *C*, rate of depletion of flow-stimulated ATP release. Using the multiple-stimulation protocol cells were repeatedly exposed to flow (shear of 0.32 dyne cm^{-2}) for 15 s while the interval between exposures was varied as indicated. Values represent relative increase in ALUs/maximum ALUs (1st flow exposure) for each perfusion. Desensitization is not observed with 5 min intervals between exposures (●), but increases as the interval between exposures is shortened to 3 min (○), 1 min (▼), and 40 s (△). Each data point represents the mean of 4–10 trials and fitted by 1st order linear regression.

reduction in the magnitude of flow-stimulated ATP release ($n = 6$, $P < 0.01$, Fig. 6*A*). To determine if these effects were through effects on the RRP of ATP, the multiple-stimulation protocol (shear of 0.32 dyne cm^{-2} for 15 s, repeated every 1 min) was utilized. Both chelerythrine and the myristoylated PKCζ pseudosubstrate significantly accelerated the rate of depletion of the RRP (relative decrease of 0.39 ALUs per perfusion for each) compared with control cells (relative decrease of 0.24 ALUs per perfusion, $n = 6$ each, $P < 0.05$, Fig. 6*B*). Together, these findings demonstrate that PKCζ regulates flow-stimulated ATP release and suggests that this is primarily through effects on a RRP.

Flow-stimulated Ca^{2+} signalling is dependent on PKC

Given that inhibition of PKCζ blocked flow-stimulated ATP release, chelerythrine and the PKCζ peptide inhibitor should have similar effects to extracellular ATP hydrolysis (apyrase) on flow-stimulated Ca^{2+} signalling. To test this hypothesis, cells were pre-incubated with either chelerythrine (1 μM for 5 min), myristoylated PKCζ pseudosubstrate, or a scrambled myristoylated PKCζ pseudosubstrate as control (10 μM for 5 min each), loaded with fura-2 and exposed to flow (shear of 0.09 dyne cm^{-2}). Exposure to flow increased $[Ca^{2+}]_i$ to 421 ± 52 nM in control cells (no treatment) and to 356 ± 101 nM in control cells treated with the scrambled peptide ($n = 3$ each, Fig. 7*A* and *F*) compared to an increase to only 42 ± 6 nM in the presence of chelerythrine ($n = 7$, $P < 0.05$) and 40 ± 7 nM in the presence of PKCζ pseudosubstrate ($n = 6$, $P < 0.05$, Fig. 7*B*,*C*,*F*). However, while overnight incubation with PMA, to down-regulate conventional and novel PKC isoforms, had no effect on shear-stimulated ATP release, it significantly blocked the increase in shear-stimulated $[Ca^{2+}]_i$ to only 19 ± 3 nM ($n = 5$, $P < 0.01$, Fig. 7*D* and *F*). This suggests the potential involvement of a phorbol ester-sensitive PKC isoform in the pathway between P2Y receptor binding and the increase in $[Ca^{2+}]_i$. To test this more directly, the effects of inhibition of atypical PKCζ (myristoylated PKCζ pseudosubstrate) *versus* inhibition of conventional and novel PKC isoforms (PMA for 18 h) were evaluated on *ATP-induced* fura-2 fluorescence in the absence of flow. In control cells, exposure to ATP (100 nM) results in characteristic increases in $[Ca^{2+}]_i$ (789 ± 141 nM, $n = 5$,

Fig. 7*E* and *F*). In the presence of the myristoylated PKCζ pseudosubstrate (10 μM), the ATP-stimulated increase in fura-2 fluorescence was unaffected (997 ± 215 nM, $n = 4$, $P =$ n.s. *versus* control), while pre-exposure to PMA (for 18 h) significantly inhibited the Ca^{2+} signal (16 ± 6 nM, $n = 4$, $P < 0.01$, Fig. 7*E* and *F*). These studies confirm that the regulatory effects of atypical and *phorbol-insensitive* PKCζ are predominantly on shear-stimulated ATP release, and suggest that other *phorbol-sensitive* isoforms are involved in the pathway between ATP–P2Y receptor binding and release of Ca^{2+} from intracellular stores.

Flow activates membrane Cl^- currents

In Mz-Cha-1 biliary cells, P2 receptor binding by ATP results in a large increase in membrane Cl^- conductance (Feranchak *et al.* 1999; Roman *et al.* 1999). To determine if mechanical flow can stimulate similar Cl^- currents, whole-cell patch clamp studies were performed in the presence or absence of flow. Under basal conditions with standard intra- and extracellular buffers, I_{Cl} was small (-0.8 ± 0.2 pA pF^{-1}, Fig. 8). Exposure to flow (shear of 0.24 dyne cm^{-2}) resulted in activation of currents within 95 ± 23 s (representative trace shown in Fig. 8*A*), increasing current density to 4.4 ± 1.2 at 0 mV ($P < 0.05$) and -14.0 ± 0.9 pA pF^{-1} at -80 mV ($P < 0.001$, $n = 9$ for each). The currents measured at 0 mV were transient and of small magnitude, while the currents measured at -80 mV were sustained for the duration of flow exposure and were fully reversible within 5 min of ceasing flow. These large flow/shear-stimulated currents exhibited reversal near 0 mV (E_{Cl}), outward rectification and time-dependent inactivation at depolarizing potentials above +60 mV (Fig. 8*A* and *B*), characteristics associated with ATP-stimulated Cl^- currents previously described in these cells (Roman *et al.* 1999). As a non-selective cation (NSC) conductance could also exhibit a reversal potential at 0 mV, additional studies were performed to establish that the flow-stimulated currents measured at -80 mV were mediated by Cl^-. First, replacement of the extracellular and intracellular monovalent cations by NMDG and TEA, respectively, did not affect the magnitude (-12.1 ± 3.2 pA pF^{-1} at -80 mV, $n = 4$, $P =$ n.s. *versus* control) or reversal potential of the flow/shear-induced currents, thus excluding a contribution from an NSC conductance (Fig. 8*C*–*E*). Second, in the presence of the Cl^- channel blocker 5-nitro-2-(3-phenylpropylamino)-benzoic acid (NPPB, 100 μM) flow-stimulated currents were significantly inhibited (-1.6 ± 0.2 pA pF^{-1} at -80 mV, $P < 0.05$, $n = 4$, Fig. 8*E*). Together these findings confirm that flow/shear activates a primary Cl^- conductance.

Flow-stimulated Cl^- currents are mediated by extracellular ATP and regulated by PKC

To determine if flow-stimulated Cl^- currents are dependent on activation of membrane P2 receptors by

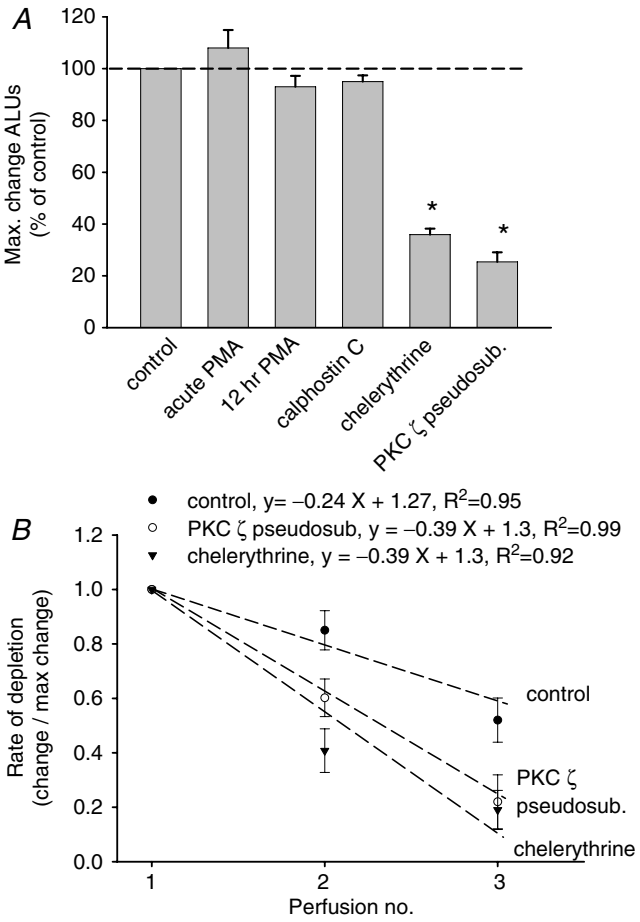

Figure 6. Inhibition of atypical PKCζ attenuates flow-stimulated ATP release

A, in separate studies the individual effects of a panel of PKC inhibitors, acute PMA (1 μM, 5 min prior to flow), 12 h PMA (1 μM for 12 h), calphostin C (500 nM), chelerythrine (1 μM), scrambled myristoylated PKC pseudosubstrate (10 μM), and myristoylated PKC pseudosubstrate (10 μM), on flow-stimulated ATP release, as assessed by the real-time L–L assay, were evaluated. Values represent percentage change in maximal ATP release within 1 min of flow exposure (shear of 0.32 dyne cm^{-2}) from control cells ($n = 5$–10 for each). Note: PKCζ pseudosubstrate value represents percentage change from the scrambled PKCζ control peptide. *Chelerythrine and myristoylated PKCζ pseudosubstrate inhibitor significantly inhibit the magnitude of flow-stimulated ATP release ($P < 0.05$ and < 0.01, respectively). *B*, inhibition of PKC affects the rate of depletion of the ATP RRP. Utilizing the multiple-stimulation protocol (Methods), cells were exposed to repetitive flow exposures (shear of 0.32 dyne cm^{-2} for 15 s) every 1 min. Values represent relative increase in ALUs/maximum ALUs (1st flow exposure) for each perfusion. Best fit line generated by 1st order linear regression. Pre-incubation with chelerythrine (▼) or myristoylated PKCζ pseudosubstrate inhibitor (-○-) results in an increase in the rate of desensitization, or depletion, of the RRP as compared to control cells (-●-) (each point mean ± S.E.M. for 6–8 trials).

extracellular ATP, studies were performed with equal concentrations of the P2 receptor antagonist suramin (100 μM) in the bath and perfusate. In the presence of suramin, the response to flow (shear of 0.24 dyne cm^{-2}) was inhibited, with a maximum Cl^- current density of -3.7 ± 1.3 pA pF^{-1} at -80 mV ($n = 6$, $P < 0.001$, Fig. 9*A* and *B*). Additionally, flow-stimulated Cl^- currents were dependent on Ca^{2+} as simultaneous removal of Ca^{2+} from the patch pipette (EGTA, 2 mM) and bath (EGTA, 1 mM) blocked currents with a maximum Cl^- current density of

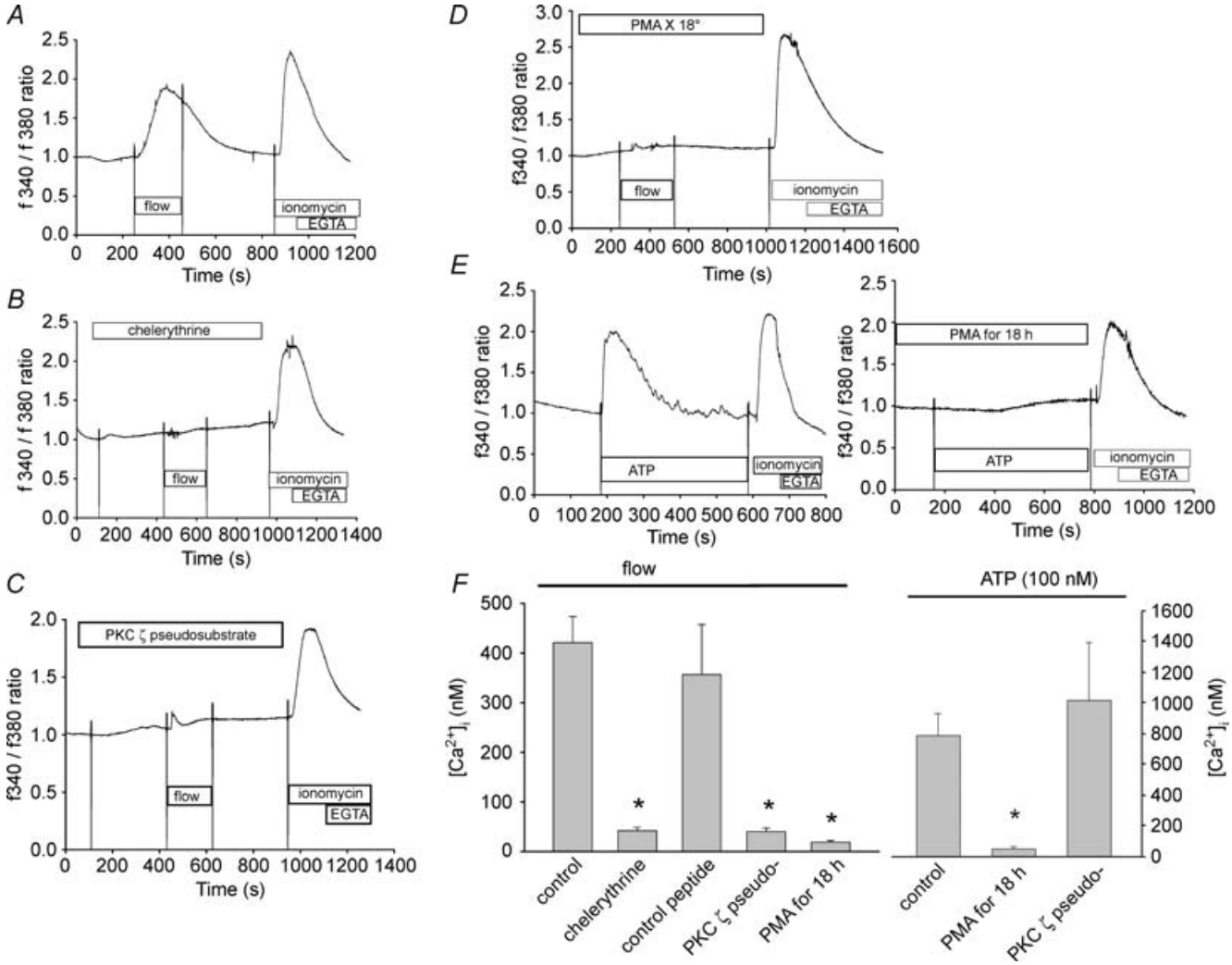

Figure 7. Flow-stimulated increases in $[Ca^{2+}]_i$ are dependent on several PKC isoforms
Mz-Cha-1 cells were incubated with either chelerythrine (1 μM for 5 min), myristoylated PKCζ pseudosubstrate, or scrambled myristoylated PKCζ peptide (10 μM for 5 min each), loaded with fura-2, and exposed to shear of 0.09 dyne cm^{-2} as indicated by the bar. *A*, representative control study demonstrating the increase in $[Ca^{2+}]_i$ associated with flow. *B*, chelerythrine blocks the flow-stimulated increase in $[Ca^{2+}]_i$, but did not affect the maximal $[Ca^{2+}]_i$ in response to ionomycin (2 μM). *C*, the myristoylated PKCζ pseudosubstrate blocked the increase in flow-stimulated fura-2 fluorescence. In some trials a small early peak in fluorescence was observed (as shown in this example). *D*, incubation (for 18 h) with PMA, to down-regulate activity of novel and conventional PKC isoforms, significantly inhibited flow-stimulated fura-2 fluorescence. *E*, in the absence of flow, ATP (100 nM) stimulates a large increase in $[Ca^{2+}]_i$. Incubation with PMA for 18 h abolishes the ATP-stimulated increase in $[Ca^{2+}]_i$. *F*, cumulative data demonstrating the individual effects of a panel of isoform selective PKC inhibitors (chelerythrine, scrambled myristoylated PKCζ peptide (control peptide) and myristoylated PKCζ pseudosubstrate peptide) on flow-stimulated (shear of 0.09 dyne cm^{-2}), and ATP-stimulated, $[Ca^{2+}]_i$. Values represent the maximal increase in $[Ca^{2+}]_i$ reported as nM ($n = 3$–7 for each). *Chelerythrine, myristoylated PKCζ pseudosubstrate and PMA for 18 h significantly inhibit the magnitude of flow-stimulated fura-2 fluorescence, while PMA for 18 h significantly inhibits the magnitude of ATP-stimulated fura-2 fluorescence.

-0.8 ± 0.3 pA pF^{-1} ($n = 4$, $P < 0.001$, data not shown). To determine the relative contributions of intra- *versus* extracellular Ca^{2+} to shear-stimulated Cl^- currents, Ca^{2+} was individually removed from either the pipette (EGTA, 2 mM) or bath (EGTA, 1 mM) and Cl^- currents measured in response to shear (0.24 dyne cm^{-2}). While removal of extracellular Ca^{2+} had little effect on the magnitude of Cl^- currents (-14.1 ± 4.1 pA pF^{-1}, $n = 5$, $P =$ n.s.), removal of intracellular Ca^{2+} significantly decreased shear-stimulated Cl^- currents (-6.5 ± 1.9 pA pF^{-1}, $n = 3$, $P < 0.05$). Lastly, to determine if flow/shear-stimulated Cl^- currents are dependent on PKC, whole-cell currents were measured in the presence or absence of the PKC inhibitor chelerythrine. In control cells, exposure to flow (shear of 0.24 dyne cm^{-2}) resulted in characteristic Cl^- currents -16.1 ± 1.7 pA pF^{-1} ($n = 7$); however, in

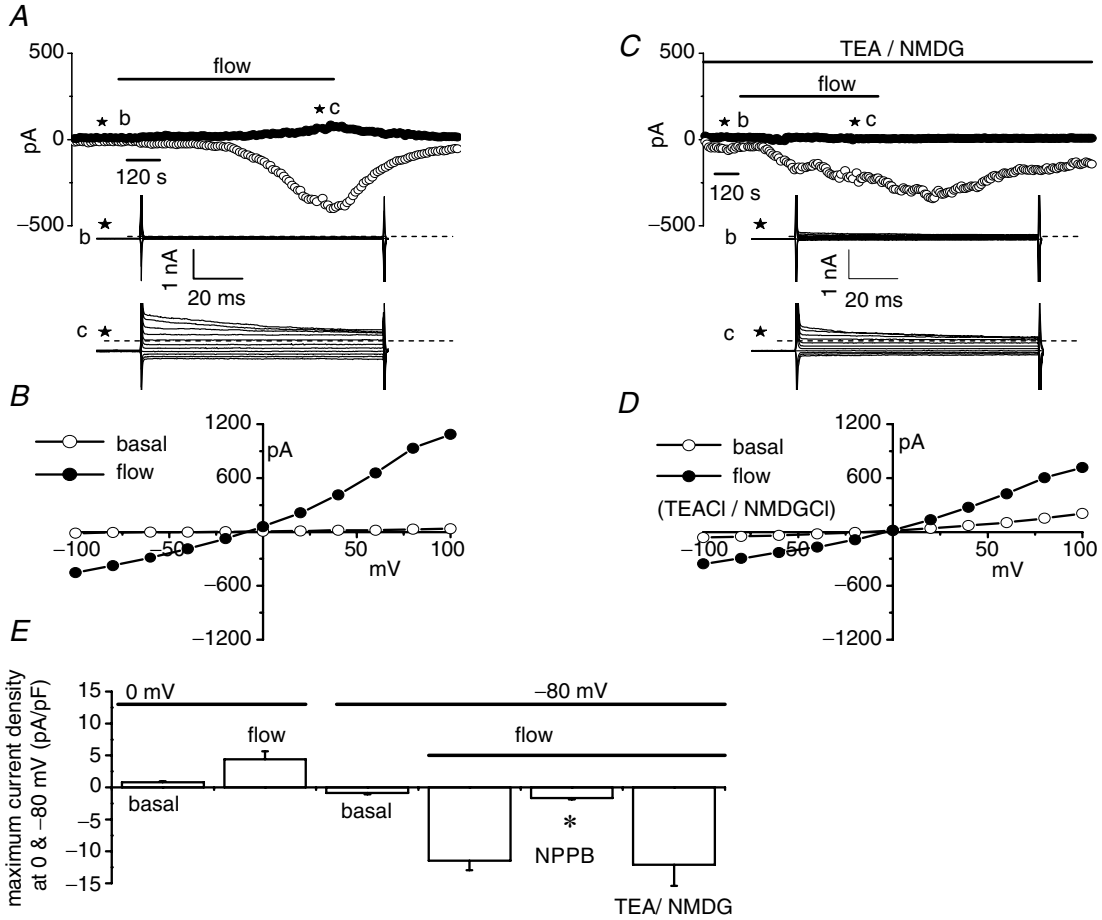

Figure 8. Exposure to flow stimulates currents in human biliary epithelial cells
Whole-cell currents were measured during basal conditions and during exposure to flow of isotonic extracellular buffer (Methods). *A*, representative whole-cell recording. Currents measured at −80 mV (○), representing I_{Cl}, and at 0 mV (●), representing I_K, are shown. Flow exposure (shear of 0.24 dyne cm^{-2}) is indicated by the bar. Currents activated within 2 min of the onset of flow and were reversible when flow was stopped. A voltage-step protocol (test potentials between −100 mV and +100 mV in 20 mV increments) was obtained at b★ (basal) and c★ (maximal current response) as indicated. Currents demonstrated time-dependent inactivation at membrane potentials > 60 mV. Zero current levels indicated by dotted lines. The *I–V* plot shown in *B* was generated from these protocols. *B*, *I–V* relationship of whole-cell currents during basal (-○-) and flow-stimulated (-●-) conditions. *C*, representative whole-cell recording demonstrating that removal of monovalent cations from the bath (NMDG) and pipette (TEA) had no effect on the magnitude of flow-stimulated currents measured at −80 mV. A voltage-step protocol (test potentials between −100 mV and +100 mV in 20 mV increments) was obtained at b★ (basal) and c★ (maximal current response) as indicated. *D*, *I–V* relationship of whole-cell currents during basal (-○-) and flow-stimulated (-●-) conditions after removal of monovalent cations from the bath and pipette (TEA·Cl/NMDG·Cl). *E*, cumulative data demonstrating magnitude of flow-stimulated currents in the presence or absence of the Cl^- channel inhibitor NPPB (100 μM) or removal of monovalent cations (TEA/NMDG). Values represent maximum current density (pA pF^{-1}) measured at 0 mV and at −80 mV ($n = 5$ each). *Flow-stimulated currents measured at −80 mV were significantly inhibited by NPPB.

the presence of chelerythrine (1 μM), the response to flow/shear was significantly inhibited with a maximum Cl^- current density of -5.5 ± 1.2 pA pF^{-1} at -80 mV ($n = 5$, $P < 0.01$, Fig 9*C* and *D*). Unfortunately, we were unable to directly assess the effects of specific PKCζ inhibition on flow-stimulated currents as the myristoylated PKCζ pseudosubstrate interfered with pipette seal formation. Together these studies demonstrate that flow/shear activates whole-cell Cl^- currents that are dependent on extracellular ATP and intracellular Ca^{2+} and are regulated by PKC. To our knowledge these studies represent the first identification of mechanosensitive Cl^- currents activated by flow in biliary epithelium.

Discussion

The key findings of the present studies in a human biliary model are: (1) fluid flow results in an increase in cellular ATP release; (2) ATP release is directly related to shear, depends on intracellular Ca^{2+}, and exhibits desensitization

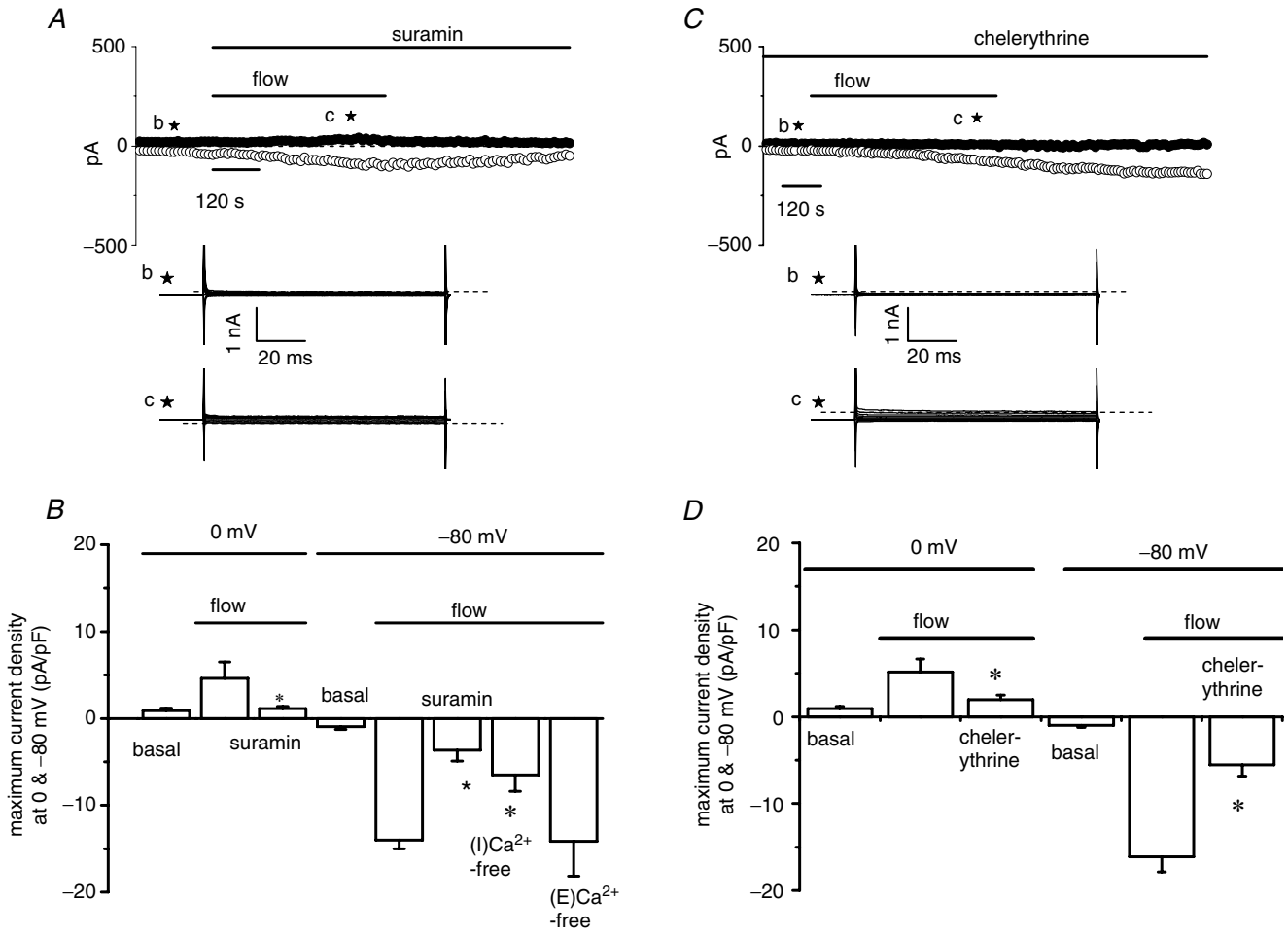

Figure 9. Flow-stimulated currents are dependent on P2 receptor stimulation and PKC
Whole-cell patch clamp studies were performed according to the protocol described in Fig. 8. *A*, representative whole-cell patch clamp recording of flow-stimulated currents (shear of 0.24 dyne cm^{-2}) in the presence of the P2 receptor antagonist suramin (100 μM). Currents measured at -80 mV (○), representing I_{Cl} and at 0 mV (●), representing I_K, are shown. In the presence of suramin, flow/shear failed to activate currents. *B*, cumulative data. *Suramin significantly ($P < 0.001$) inhibited flow-stimulated currents ($n = 6$). *†Removal of intracellular Ca^{2+} ((I)Ca^{2+}-free; EGTA, 2 mM, in pipette solution) significantly inhibited the magnitude of flow-stimulated currents ($n = 3$, $P < 0.01$), while removal of extracellular Ca^{2+} ((E)Ca^{2+}-free; EGTA, 1 mM, in extracellular buffer) had no effect ($n = 5$, $P =$ n.s.). Values represent maximum current density (pA pF^{-1}) measured at 0 mV and -80 mV. *C*, representative whole-cell current recording demonstrating that inhibition of PKC by chelerythrine (1 μM) inhibits flow-stimulated currents. *D*, cumulative data demonstrating effect of chelerythrine on flow-stimulated currents. Values represent maximum current density (pA pF^{-1}) measured at 0 mV and -80 mV, respectively ($n = 5$ each). *Chelerythrine significantly inhibited flow-stimulated currents ($P < 0.01$).

with repeated flow exposures; (3) fluid flow increases $[Ca^{2+}]_i$ in part through ATP release and stimulation of membrane P2Y receptors; (4) flow-stimulated ATP release is regulated by atypical PKCζ; and (5) flow activates membrane Cl^- currents through effects on extracellular ATP and increases in $[Ca^{2+}]_i$. Together these findings suggest that the mechanical force of flow itself may directly regulate cholangiocyte secretion and bile formation. Thus, these studies describe for the first time, a potential role of mechanical force in the regulation of biliary epithelial function. While the role of mechanotransduction in physiological functions in specialized cell types, such as sensory cells of the ear or mechanoreceptors in the skin, is well established, the role of mechanical stresses in epithelial cell transport is continuing to expand. For example, in renal epithelial cells flow appears to mediate Ca^{2+} influx through a pathway involving PC-1 and PC-2 (Nauli *et al.* 2003) and in the renal tubule, mechanical flow and/or distention modulates the epithelial Na^+ channel (ENaC) through effects on channel open probability (Satlin *et al.* 2001; Morimoto *et al.* 2006). Additionally, in respiratory epithelial cells, phasic shear stress appears to modulate the volume and composition of airway surface fluid (Tarran *et al.* 2005, 2006). Our studies provide initial evidence that mechanical force modulates biliary epithelial cell transport. Elucidating the mechanotransduction pathways in biliary epithelium may provide new insight into cholangiocyte function and suggest new strategies for regulating bile formation.

Based on these findings and our previously published work (Feranchak *et al.* 1999; Roman *et al.* 1999), we propose a working model whereby mechanical effects of flow are transduced to cholangiocyte ATP release, P2 receptor binding, increases in $[Ca^{2+}]_i$ and Cl^- secretion (Fig. 10). Flow-stimulated ATP release therefore serves as a choleretic by binding apical P2 receptors and stimulating membrane Ca^{2+}-activated Cl^- channels (Schlenker *et al.* 1997; Roman *et al.* 1999). In this way, a rise in the shear force at the apical cholangiocyte membrane, through increases in flow rate or bile viscosity, may stimulate ATP release and hence result in changes in bile composition. For example, bile acid secretion across the hepatocyte canalicular membrane increases both bile acid-dependent flow rate and bile viscosity which, according to our proposed model, would increase downstream cholangiocyte ATP release through mechanical effects at the apical membrane. Flow-stimulated ATP release would serve as an autocrine/paracrine signal, ultimately resulting in bile dilution and alkalinization. If our proposed model applies to *in vivo* conditions, it may represent an attractive mechanism to increase biliary secretion, and hence dilute bile in response to bile acid-dependent increases in bile flow or viscosity. Therefore this becomes a 'feed forward' pathway and may help to explain the hypercholeresis, out of proportion to bile acid-induced bile flow alone, observed with bile acid replacement therapy (Scharschmidt & Lake, 1989), and suggests a possible mechanism for the increase in Ca^{2+}-activated Cl^- channel activity observed in cholangiocytes in response to ursodeoxycholic acid exposure (Shimokura *et al.* 1995).

Since the flow rate and shear force generated in the intrahepatic bile ducts are not amenable to direct assessment, the flow rates used in this study were based on observations, as well as calculations, derived from previous studies of animal models. To determine the

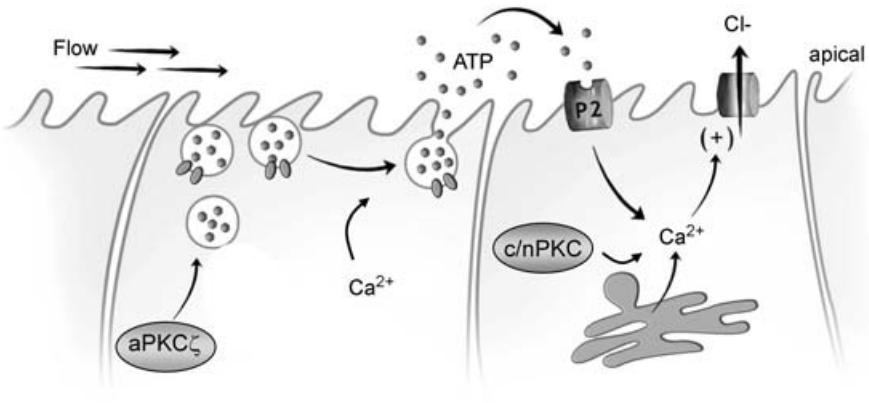

Figure 10. Proposed model of flow-stimulated ATP release and P2 signalling in biliary epithelium
The force of flow results in ATP release from biliary cells through a mechanism that is dependent on atypical PKCζ and intracellular Ca^{2+}. The cellular mechanism of regulated ATP release is unknown, but may involve exocytosis of ATP-enriched vesicles, ATP-channel insertion, or a combination of pathways. Released ATP binds P2 receptors in an autocrine or paracrine manner resulting in an increase in intracellular Ca^{2+}, through a mechanism involving conventional and/or novel PKC isoforms, and Cl^- channel activation. The molecular identity of the specific P2 receptor subtype(s) and the Cl^- channel involved are unknown. aPKCζ, atypical PKCζ; c/n PKC, conventional and novel PKC isoforms.

flow rates in smaller ducts, Masyuk *et al.* utilized a computerized tomography scanning (micro-CT) method with 3-dimensional reconstruction of the rat biliary tree to evaluate bile duct size and then used mathematical calculations to estimate flow rates (Masyuk *et al.* 2004). Based on these calculations the estimated flow rate was 11.1 nl min^{-1} in small bile ducts (50 μm) and 1064 nl min^{-1} in the larger ducts (225 μm) corresponding to a shear force of $\sim$0.14 dyne cm^{-2}. It should be noted that these calculations are based on Murray's law (Murray, 1926), which utilizes a constant value for viscosity and hence presumes wall shear stress is constant throughout the system. These assumptions may not directly apply to the branching biliary network where differences in bile viscosity may potentially exist between different duct segments. While our present studies utilized shear forces within this calculated range, direct evaluation of flow rates and shear force in the small intrahepatic bile ducts will have to await technical advances.

If these studies, performed in a human biliary epithelial model, translate to *in vivo* conditions, several points, as well as uncertainties, deserve highlighting. First, the identity of the mechanosensor(s), which transduce membrane flow force to ATP release are unknown. Recently, the importance of the primary cilium as a flow sensor in epithelial cells has been demonstrated (Praetorius & Spring, 2003; Huang *et al.* 2006). In fact, in rat bile duct segments, deflections of the primary cilium by flow result in a rapid increase in $[Ca^{2+}]_i$ (Masyuk *et al.* 2006). While the NRC express a primary cilium at the apical membrane, the Mz-Cha-1 biliary cells do not express a cilium at any time point in their development, including the time points at which the ATP release experiments were performed (Supplemental Fig. 1.2). This suggests that flow/shear-stimulated ATP release can occur through *cilium-independent* means. In fact, flow-stimulated ATP release has been shown to occur in endothelial cells that do not express a cilium (Yamamoto *et al.* 2000; Iomini *et al.* 2004), and in MDCK cells which do express a cilium, mechanosensitive ATP release can occur in response to different stimuli through both cilium-dependent and -independent pathways (Praetorius *et al.* 2005). Thus, cilium-independent mechanosensitive ATP release appears to occur in several cell types. While the present studies demonstrate that flow/shear-stimulated ATP release may occur through cilium-independent pathways, they do not discount a potential contribution of the primary cilium to mechanosensitive ATP release. In fact, it is interesting to note that for a given shear, the primary cilium-expressing NRC monolayers demonstrate a greater relative increase in ATP release than the Mz-Cha-1 cells. Further studies to characterize the role of the primary cilium in cholangiocyte ATP release, as well as to identify other potential mechanosensor(s) involved in P2 signalling, are clearly indicated.

Second, the cellular mechanism of ATP release is unknown. While previous studies in a variety of epithelial cells have emphasized a potential channel-mediated pathway (Reisin *et al.* 1994; Cotrina *et al.* 1998; Okada *et al.* 2004), no definitive evidence exists establishing the molecular identity for an ATP channel in epithelial cells. Conversely, there is increasing indirect evidence that vesicular exocytosis contributes to epithelial ATP release. For example, previous studies of Mz-Cha-1 cells have demonstrated that cell swelling is associated with parallel increases in both the rate of exocytosis and ATP release through a process requiring Ca^{2+} and PKC (Gatof *et al.* 2004). Interestingly, PKC has been shown to increase the size of the RRP of secretory granules in chromaffin cells (Gillis *et al.* 1996). Our present studies therefore, demonstrating that (i) ATP release is dependent on intracellular Ca^{2+} and PKC, (ii) the pool of ATP becomes depleted with repetitive flow-stimulation, and (iii) inhibition of PKC accelerates the rate of depletion, together provide further evidence of the existence of an ATP-enriched vesicular compartment. These studies, however, are indirect, and while flow has been shown to modulate both PKC activity (Tseng *et al.* 1995) and the rate of exocytosis (Apodaca, 2002) in other cell models, the specific mechanism mediating flow-stimulated ATP release in biliary epithelium will require further study.

Third, while the present studies demonstrate that *flow/shear-stimulated* ATP release is regulated in part by atypical PKCζ, previous studies of Mz-Cha-1 biliary cells have demonstrated that *volume-stimulated* ATP release is both calcium- and phorbol ester-sensitive (Gatof *et al.* 2004), suggesting involvement of conventional PKC isoform(s). Taken together, these findings suggest that a diversity of PKC isoforms may be involved in mechanosensitive signalling, with different isoforms responding to different mechanical stimuli (cell swelling *versus* flow/shear). Elucidation of the specific PKC isoforms, as well as other kinase signalling pathways involved in mechanosensitive biliary functions, will require significant further study.

Fourth, the cellular pathways regulating mechanosensitive Ca^{2+} signalling in biliary epithelium have not been fully elucidated. Flow has been shown to be a potent stimulus increasing intracellular Ca^{2+} in several epithelial models (Praetorius & Spring, 2001; Woda *et al.* 2002; Nauli *et al.* 2003; Liu *et al.* 2005*b*), including biliary epithelium (Masyuk *et al.* 2006). While these effects appear to be mediated through mechanical effects on the primary cilium (Praetorius & Spring, 2003), some cells increase Ca^{2+} in response to flow in the absence of cilium expression (Liu *et al.* 2003) and alternate pathways involving P2 receptors have recently emerged as potential contributors to the response (Jensen *et al.* 2007). Interestingly, in the rat isolated bile duct model, while the flow-stimulated increase in Ca^{2+} is abolished after

the cilium is removed (via chloral hydrate), the cells still demonstrate an increase in intracellular Ca^{2+} in response to exogenous ATP delivered to the luminal membrane (Masyuk *et al.* 2006). The Mz-Cha-1 cells do not express a primary cilium and hence the flow-stimulated increase in Ca^{2+} observed at higher flow rates in this cell type must take place through a cilium-independent pathway. This is further substantiated by the findings that the flow-stimulated Ca^{2+} signal is abolished in the presence of apyrase or suramin confirming that extracellular ATP and P2 receptor stimulation are required. Thus, cholangiocytes demonstrate several mechanosensitive pathways that regulate intracellular Ca^{2+}, both cilium-dependent and -independent. Indeed, cholangiocytes express a host of membrane Ca^{2+} transport proteins including polycystin-1 and -2 (Masyuk *et al.* 2006), fibrocystin (Ward *et al.* 2003), TRPV4 (Gradilone *et al.* 2007), P2X7 (Taylor *et al.* 1999), and P2X4 receptors (Doctor *et al.* 2005). The expression, regulation and mechanical sensitivity of these channels and transporters in biliary epithelium are only beginning to be elucidated.

Fifth, while the present studies support a role for ATP binding P2 receptors in flow-stimulated Ca^{2+} signalling and Cl^- transport, the specific P2X and P2Y subtypes involved are unknown. Cholangiocytes express a repertoire of both P2X and P2Y receptors on the apical membrane (Schlenker *et al.* 1997; Taylor *et al.* 1999; Dranoff *et al.* 2001; Doctor *et al.* 2005) which may vary to meet changing physiological demands. Indeed, cholangiocytes demonstrate a rapid rate of constitutive exo- and endocytosis capable of replacing 1.3% of the plasma membrane, along with specific membrane proteins (e.g. ion channels, receptors), every minute (Fitz, 2002; Doctor *et al.* 2002). The number, type and location of P2 receptors present at any given moment, therefore, may be an important determinant of cholangiocyte transport. Flow/shear-dependent changes in P2 receptor expression have been demonstrated in endothelial cells (Korenaga *et al.* 2001). Additionally, the findings of abnormal flow-induced Ca^{2+} responses in the endothelium of a P2X4−/− mouse model (Yamamoto *et al.* 2006) and in the renal tubule of a P2Y2−/− mouse model (Jensen *et al.* 2007) further highlight the importance of P2 receptors in mediating cellular responses to mechanical forces. The role of fluid flow and other mechanical stimuli in the expression and regulation of cholangiocyte cell surface P2 receptors is therefore an exciting area for further investigation.

Sixth, while ATP is always found in bile in low micromolar concentrations (Chari *et al.* 1996), suggesting a significant constitutive release exists; the physiological relevance to bile formation is unknown. However, the finding that addition of apyrase, to rapidly hydrolyse ATP, to rat cholangiocyte monolayers mounted in an Ussing chamber decrease the short circuit current response (I_{sc}) (Roman *et al.* 1999), a reflection of transepithelial Cl^- secretion, suggests that constitutive ATP release may contribute to basal cholangiocyte secretion. In other words, a basal *purinergic tone* may exist. Additionally, utilizing cell-surface tethered luciferin–luciferase assay systems in other cell models, several investigators have shown that the concentration of ATP in the microenvironment at the cell surface may be different from that measured in bulk solution (Beigi *et al.* 1999; Okada *et al.* 2006). Therefore, while ATP may always be detected in bulk solution, a rapid increase or transient spike, in the local concentration of ATP at the cholangiocyte surface may be the stimulus to initiate P2-mediated signalling. To add additional complexity to P2 signalling, other nucleotides, such as UTP, may be released simultaneously with ATP (Tatur *et al.* 2007), via nucleotide-enriched vesicles or through separate nucleotide-permeable channels, and may further potentiate ATP release (Liu *et al.* 2005*a*) as well as contribute to the cellular secretory response.

Lastly, the molecular identity of the Cl^- channel(s) responsible for the flow-stimulated increase in Cl^- conductance is unknown. Flow-stimulated Cl^- currents have been described in endothelial cells (Gautam *et al.* 2006); and in respiratory epithelium shear stress results in changes in surface fluid volume and composition, presumably through effects on membrane Cl^- permeability (Tarran *et al.* 2005). It is interesting that the biophysical properties of the flow-stimulated Cl^- currents described here, as well as regulation by extracellular ATP, are similar to the cell swelling-activated Cl^- channel previously described in these cells (Feranchak *et al.* 1999; Roman *et al.* 1999) suggesting the existence of a mechanosensitive P2 receptor–channel complex capable of responding to various plasma membrane-directed forces. Thus, the 'extracellular nucleotide–P2 receptor–Cl^- channel' signalling complex may represent an important mechanotransduction pathway linking external physical forces to membrane ion permeability and cellular metabolism.

In conclusion, these are the first studies to identify a physiological stimulus for biliary ATP release. The finding that flow stimulates ATP release is novel and suggests that the mechanical force of flow itself is a potential regulator of bile composition. Additionally, these are the first studies to identify mechanosensitive Cl^- channels activated by flow in biliary epithelial cells. Understanding the pathways involved in mechanosensitive ATP release, Ca^{2+} signalling and ion transport may provide novel insight into the regulation of biliary secretion and suggest new and innovative strategies for the treatment of cholestatic liver disorders.

References

Apodaca G (2002). Modulation of membrane traffic by mechanical stimuli. *Am J Physiol Renal Physiol* **282**, F179–F190.

Basavappa S, Middleton JP, Mangel A, McGill J, Cohn JA & Fitz JG (1993). Cl^- and K^+ transport in human biliary cell lines. *Gastroenterology* **104**, 1796–1805.

Beigi R, Kobatake E, Aizawa M & Dubyak GR (1999). Detection of local ATP release from activated platelets using cell surface-attached firefly luciferase. *Am J Physiol Cell Physiol* **276**, C267–C278.

Bodin P & Burnstock G (2001). Evidence that release of adenosine triphosphate from endothelial cells during increased shear stress is vesicular. *J Cardiovasc Pharmacol* **38**, 900–908.

Chang D, Hsieh PS & Dawson DC (1988). Calcium: a program in basic for calculating the composition of solutions with specified free concentrations of calcium, magnesium and other divalent cations. *Comput Biol Med* **18**, 351–366.

Chari RS, Schutz SM, Haebig JA, Shimokura GH, Cotton PB, Fitz JG & Meyers WC (1996). Adenosine nucleotides in bile. *Am J Physiol Gastrointest Liver Physiol* **270**, G246–G252.

Chen NX, Ryder KD, Pavalko FM, Turner CH, Burr DB, Qiu J & Duncan RL (2000). Ca^{2+} regulates fluid shear-induced cytoskeletal reorganization and gene expression in osteoblasts. *Am J Physiol Cell Physiol* **278**, C989–C997.

Cotrina ML, Lin J, Alves-Roriguez A, Liu S, Li J, Azmi-Ghadimi H, Kang J, Naus CCG & Nedergaard M (1998). Connexins regulate calcium signaling by controling ATP release. *Proc Nat Acad Sci U S A* **95**, 15735–15740.

Doctor RB, Dahl R, Fouassier L, Kilic G & Fitz JG (2002). Cholangiocytes exhibit dynamic, actin-dependent apical membrane turnover. *Am J Physiol Cell Physiol* **282**, C1042–C1052.

Doctor RB, Matzakos T, McWilliams R, Johnson S, Feranchak AP & Fitz JG (2005). Purinergic regulation of cholangiocyte secretion: identification of a novel role for P2X receptors. *Am J Physiol Gastrointest Liver Physiol* **288**, G779–G786.

Dranoff JA, Masyuk AI, Kruglov EA, LaRusso NF & Nathanson MH (2001). Polarized expression and function of P2Y ATP receptors in rat bile duct epithelia. *Am J Physiol Gastrointest Liver Physiol* **281**, G1059–G1067.

Dull RO & Davies PF (1991). Flow modulation of agonist (ATP)-response (Ca^{2+}) coupling in vascular endothelial cells. *Am J Physiol* **261**, H149–H154.

Farias M III, Gorman MW, Savage MV & Feigl EO (2005). Plasma ATP during exercise: possible role in regulation of coronary blood flow. *Am J Physiol Heart Circ Physiol* **288**, H1586–H1590.

Feranchak AP, Berl T, Capasso J, Wojtaszek PA, Han J & Fitz JG (2001). p38 MAP kinase modulates liver cell volume through inhibition of membrane Na^+ permeability. *J Clin Invest* **108**, 1495–1504.

Feranchak AP, Doctor RB, Troetsch M, Brookman K, Johnson SM & Fitz JG (2004). Calcium-dependent regulation of secretion in biliary epithelial cells: the role of apamin-sensitive SK channels. *Gastroenterology* **127**, 903–913.

Feranchak AP & Fitz JG (2002). Adenosine triphosphate release and purinergic regulation of cholangiocyte transport. *Semin Liver Dis* **22**, 251–262.

Feranchak AP, Fitz JG & Roman RM (2000). Volume-sensitive purinergic signaling in human hepatocytes. *J Hepatol* **33**, 174–182.

Feranchak AP, Roman RM, Doctor RB, Salter KD, Toker A & Fitz JG (1999). The lipid products of phosphoinositide 3-kinase contribute to regulation of cholangiocyte ATP and chloride transport. *J Biol Chem* **274**, 30979–30986.

Feranchak AP, Roman RM, Schwiebert EM & Fitz JG (1998). Phosphatidyl inositol 3-kinase represents a novel signal regulating cell volume through effects on ATP release. *J Biol Chem* **273**, 14906–14911.

Fitz JG (1996). Cellular mechanisms of bile secretion. In *Hepatology*, ed. Zakim D & Boyer TD, pp. 362–376. W.B. Saunders Company, Philadelphia.

Fitz JG (2002). Regulation of cholangiocyte secretion. *Semin Liver Dis* **22**, 241–249.

Fitz JG & Sostman A (1994). Nucleotide receptors activate cation, potassium, and chloride currents in a liver cell line. *Am J Physiol Gastrointest Liver Physiol* **266**, G544–G553.

Gatof D, Kilic G & Fitz JG (2004). Vesicular exocytosis contributes to volume-sensitive ATP release in biliary cells. *Am J Physiol Gastrointest Liver Physiol* **286**, G538–G546.

Gautam M, Shen Y, Thirkill TL, Douglas GC & Barakat AI (2006). Flow-activated chloride channels in vascular endothelium: Shear stress sensitivity, desensitization dynamics, and physiological implications. *J Biol Chem* **281**, 36492–36500.

Genetos DC, Geist DJ, Liu D, Donahue HJ & Duncan RL (2005). Fluid shear-induced ATP secretion mediates prostaglandin release in MC3T3-E1 osteoblasts. *J Bone Miner Res* **20**, 41–49.

Gillis KD, Mossner R & Neher E (1996). Protein kinase C enhances exocytosis from chromaffin cells by increasing the size of the readily releasable pool of secretory granules. *Neuron* **16**, 1209–1220.

Gradilone SA, Masyuk AI, Splinter PL, Banales JM, Huang BQ, Tietz PS, Masyuk TV & LaRusso NF (2007). Cholangiocyte cilia express TRPV4 and detect changes in luminal tonicity inducing bicarbonate secretion. *Proc Natl Acad Sci U S A* **104**, 19138–19143.

Herbert JM (1990). Chelerythrine is a potent and specific inhibitor of protein kinase C. *Biochem Biophys Res Comm* **172**, 993–999.

Huang BQ, Masyuk TV, Muff MA, Tietz PS, Masyuk AI & LaRusso NF (2006). Isolation and characterization of cholangiocyte primary cilia. *Am J Physiol Gastrointest Liver Physiol* **291**, G500–G509.

Iomini C, Tejada K, Mo W, Vaananen H & Piperno G (2004). Primary cilia of human endothelial cells disassemble under laminar shear stress. *J Cell Biol* **164**, 811–817.

Jensen ME, Odgaard E, Christensen MH, Praetorius HA & Leipziger J (2007). Flow-induced $[Ca^{2+}]_i$ increase depends on nucleotide release and subsequent purinergic signaling in the intact nephron. *J Am Soc Nephrol* **18**, 2062–2070.

Knight GE, Bodin P, De Groat WC & Burnstock G (2002). ATP is released from guinea pig ureter epithelium on distension. *Am J Physiol Renal Physiol* **282**, F281–F288.

Knuth A, Gabbert H, Dippold W, Klein O, Sachsse W, Bitter-Suermann D, Prellwitz W & Meyer zum Buschenfelde KH (1985). Biliary Adenocarcinoma. Characterization of three new human tumor cell lines. *J Hept* **1**, 579–596.

Korenaga R, Yamamoto K, Ohura N, Sokabe T, Kamiya A & Ando J (2001). Sp1-mediated downregulation of P24 receptor gene transcription in endothelial cells exposed to shear stress. *Am J Physiol Heart Circ Physiol* **280**, H2214–H2221.

Lazaridis KN, Pham L, Tietz P, Marinelli RA, Degroen PC, Levine S, Dawson PA & LaRusso NF (1997). Rat cholangiocytes absorb bile acids at their apical domain via the ileal sodium-dependent bile acid transporter. *J Clin Invest* **100**, 2714–2721.

Lenzen R, Elster J, Behrend C, Hampel K-E, Bechstein W-O & Neuhaus P (1997). Bile acid-independent bile flow is differentially regulated by glucagon and secretin in humans after orthotopic liver transplantation. *Hepatology* **26**, 1272–1281.

Lira M, Schteingart CD, Steinbach JH, Lambert KJ, McRoberts JA & Hofmann AF (1992). Sugar absorption by the biliary ductular epithelium of the rat: evidence for two transport systems. *Gastroenterology* **102**, 563–571.

Liu GJ, Werry EL & Bennett MR (2005*a*). Secretion of ATP from Schwann cells in response to uridine triphosphate. *Eur J Neurosci* **21**, 151–160.

Liu W, Murcia NS, Duan Y, Weinbaum S, Yoder BK, Schwiebert E & Satlin LM (2005*b*). Mechanoregulation of intracellular Ca^{2+} concentration is attenuated in collecting duct of monocilium-impaired orpk mice. *Am J Physiol Renal Physiol* **289**, F978–F988.

Liu W, Xu S, Woda C, Kim P, Weinbaum S & Satlin LM (2003). Effect of flow and stretch on the $[Ca^{2+}]_i$ response of principal and intercalated cells in cortical collecting duct. *Am J Physiol Renal Physiol* **285**, F998–F1012.

Masyuk AI, Masyuk TV, Splinter PL, Huang BQ, Stroope AJ & LaRusso NF (2006). Cholangiocyte cilia detect changes in luminal fluid flow and transmit them into intracellular Ca^{2+} and cAMP signaling. *Gastroenterology* **131**, 911–920.

Masyuk TV, Masyuk AI, Ritman EL & LaRusso NF (2004). Three-dimensional reconstruction of the rat intrahepatic biliary tree: physiologic implications. In *The Pathophysiology of Biliary Epithelia*, ed. Alpini G, Alvaro D, Marzioni M, Lesage G & LaRusso N, pp. 60–71. Landes Bioscience, Georgetown, TX.

Morimoto T, Liu W, Woda C, Carattino MD, Wei Y, Hughey RP, Apodaca G, Satlin LM & Kleyman TR (2006). Mechanism underlying flow stimulation of sodium absorption in the mammalian collecting duct. *Am J Physiol Renal Physiol* **291**, F663–F669.

Murray CD (1926). The physiological principle of minimum work. I. The vascular system and the cost of blood volume. *Proc Natl Acad Sci U S A* **12**, 207–214.

Nakatsuka H, Sokabe T, Yamamoto K, Sato Y, Hatakeyama K, Kamiya A & Ando J (2006). Shear stress induces hepatocyte PAI-1 gene expression through cooperative Sp1/Ets-1 activation of transcription. *Am J Physiol Gastrointest Liver Physiol* **291**, G26–G34.

Nauli SM, Alenghat FJ, Luo Y, Williams E, Vassilev P, Li X, Elia AE, Lu W, Brown EM, Quinn SJ, Ingber DE & Zhou J (2003). Polycystins 1 and 2 mediate mechanosensation in the primary cilium of kidney cells. *Nat Genet* **33**, 129–137.

Oheim M, Loerke D, Stuhmer W & Chow RH (1999). Multiple stimulation-dependent processes regulate the size of the releasable pool of vesicles. *Eur Biophys J* **28**, 91–101.

Okada SF, Nicholas RA, Kreda SM, Lazarowski ER & Boucher RC (2006). Physiological regulation of ATP release at the apical surface of human airway epithelia. *J Biol Chem* **281**, 22992–23002.

Okada SF, O'Neal WK, Huang P, Nicholas RA, Ostrowski LE, Craigen WJ, Lazarowski ER & Boucher RC (2004). Voltage-dependent anion channel-1 (VDAC-1) contributes to ATP release and cell volume regulation in murine cells. *J Gen Physiol* **124**, 513–526.

Patel AS, Reigada D, Mitchell CH, Bates SR, Margulies SS & Koval M (2005). Paracrine stimulation of surfactant secretion by extracellular ATP in response to mechanical deformation. *Am J Physiol Lung Cell Mol Physiol* **289**, L489–L496.

Praetorius HA, Frokiaer J & Leipziger J (2005). Transepithelial pressure pulses induce nucleotide release in polarized MDCK cells. *Am J Physiol Renal Physiol* **288**, F133–F141.

Praetorius HA & Spring KR (2001). Bending the MDCK cell primary cilium increases intracellular calcium. *J Membr Biol* **184**, 71–79.

Praetorius HA & Spring KR (2003). Removal of the MDCK cell primary cilium abolishes flow sensing. *J Membr Biol* **191**, 69–76.

Reisin IL, Prat AG, Abraham EH, Amara JF, Gregory RJ, Ausiello DA & Cantiello HF (1994). The cystic fibrosis transmembrane conductance regulator is a dual ATP and chloride channel. *J Biol Chem* **269**, 20584–20591.

Roman RM, Bodily K, Wang Y, Raymond JR & Fitz JG (1998). Activation of protein kinase C alpha couples cell volume to membrane Cl^- permeability in HTC hepatoma and Mz-ChA-1 cholangiocarcinoma cells. *Hepatology* **28**, 1073–1080.

Roman RM, Feranchak AP, Salter KD, Wang Y & Fitz JG (1999). Endogenous ATP regulates Cl^- secretion in cultured human and rat biliary epithelial cells. *Am J Physiol Gastrointest Liver Physiol* **276**, G1391–G1400.

Roman RM, Wang Y & Fitz JG (1996). Regulation of cell volume in a human biliary cell line: calcium-dependent activation of K^+ and Cl^- currents. *Am J Physiol Gastrointest Liver Physiol* **271**, G239–G248.

Salter KD, Fitz JG & Roman RM (2000*a*). Domain-specific purinergic signaling in polarized rat cholangiocytes. *Am J Physiol Gastrointest Liver Physiol* **278**, G492–G500.

Salter KD, Roman RM, LaRusso NR, Fitz JG & Doctor RB (2000*b*). Modified culture conditions enhance expression of differentiated phenotypic properties of normal rat cholangiocytes. *Laboratory Invest* **80**, 1775–1778.

Satlin LM, Sheng S, Woda CB & Kleyman TR (2001). Epithelial Na^+ channels are regulated by flow. *Am J Physiol Renal Physiol* **280**, F1010–F1018.

Scharschmidt BF & Lake JR (1989). Hepatocellular bile acid transport and ursodeoxycholic acid hypercholeresis. *Dig Dis Sci* **34**, 5S–15S.

Schlenker T, Romac JMJ, Sharara A, Roman RM, Kim S, LaRusso N, Liddle R & Fitz JG (1997). Regulation of biliary secretion through apical purinergic receptors in cultured rat cholangiocytes. *Am J Physiol Gastrointest Liver Physiol* **273**, G1108–G1117.

Shimokura GH, McGill J, Schlenker T & Fitz JG (1995). Ursodeoxycholate increases cytosolic calcium concentration and activates Cl^- currents in a biliary cell line. *Gastroenterology* **109**, 965–972.

Simpson A (1999). Fluorescent measurement of $[Ca^{2+}]$. In *Methods in Molecular Biology: Calcium Signaling Protocols*, ed. Lambert D, Human Press Inc., Totowa, NJ.

Spagnou S, Miller AD & Keller M (2004). Lipidic carriers of siRNA: differences in the formulation, cellular uptake, and delivery with plasmid DNA. *Biochem* **43**, 13348–13356.

Steyer JA, Horstmann H & Almers W (1997). Transport, docking and exocytosis of single secretory granules in live chromaffin cells. *Nature* **388**, 474–478.

Sun R, Gao P, Chen L, Ma D, Wang J, Oppenheim JJ & Zhang N (2005). Protein kinase C zeta is required for epidermal growth factor-induced chemotaxis of human breast cancer cells. *Cancer Res* **65**, 1433–1441.

Tarran R, Button B & Boucher RC (2006). Regulation of normal and cystic fibrosis airway surface liquid volume by phasic shear stress. *Annu Rev Physiol* **68**, 543–561.

Tarran R, Button B, Picher M, Paradiso AM, Ribeiro CM, Lazarowski ER, Zhang L, Collins PL, Pickles RJ, Fredberg JJ & Boucher RC (2005). Normal and cystic fibrosis airway surface liquid homeostasis. The effects of phasic shear stress and viral infections. *J Biol Chem* **280**, 35751–35759.

Tatur S, Groulx N, Orlov SN & Grygorczyk R (2007). Ca^{2+}-dependent ATP release from A549 cells involves synergistic autocrine stimulation by coreleased uridine nucleotides. *J Physiol* **584**, 419–435.

Taylor AL, Kudlow BA, Marrs KL, Gruenert D, Guggino WB & Schwiebert EM (1998). Bioluminescence detection of ATP release mechanisms in epithelia. *Am J Physiol Cell Physiol* **275**, C1391–C1406.

Taylor AL, Schwiebert LM, Smith JJ, King C, Jones JR, Sorscher EJ & Schwiebert EM (1999). Epithelial P2x purinergic receptor channel expression and function. *J Clin Invest* **104**, 875–884.

Tseng H, Peterson TE & Berk BC (1995). Fluid shear stress stimulates mitogen-activated protein kinase in endothelial cells. *Circ Res* **77**, 869–878.

Ueda I, Shinoda F & Kamaya H (1994). Temperature-dependent effects of high pressure on the bioluminescence of firefly luciferase. *Biophys J* **66**, 2107–2110.

Vroman B & LaRusso N (1996). Development and characterization of polarized primary cultures of rat intrahepatic bile duct epithelial cells. *Laboratory Invest* **74**, 303–313.

Wang EC, Lee JM, Ruiz WG, von Balestreire EMBM, Barrick S, Cockayne DA, Birder LA & Apodaca G (2005). ATP and purinergic receptor-dependent membrane traffic in bladder umbrella cells. *J Clin Invest* **115**, 2412–2422.

Wang Y, Roman RM, Schlenker T, Hannun YA, Raymond JR & Fitz JG (1997). Cytosolic calcium and protein kinase Cα couple cellular metabolism to membrane K^+ permeability in a human biliary cell line. *J Clin Invest* **99**, 2890–2897.

Ward CJ, Yuan D, Masyuk TV, Wang X, Punyashthiti R, Whelan S, Bacallao R, Torra R, LaRusso NF, Torres VE & Harris PC (2003). Cellular and subcellular localization of the ARPKD protein; fibrocystin is expressed on primary cilia. *Hum Mol Genet* **12**, 2703–2710.

Woda CB, Leite M Jr, Rohatgi R & Satlin LM (2002). Effects of luminal flow and nucleotides on $[Ca^{2+}]_i$ in rabbit cortical collecting duct. *Am J Physiol Renal Physiol* **283**, F437–F446.

Yamamoto K, Korenaga R, Kamiya A & Ando J (2000). Fluid shear stress activates Ca^{2+} influx into human endothelial cells via P2X4 purinoceptors. *Circ Res* **87**, 385–391.

Yamamoto K, Sokabe T, Matsumoto T, Yoshimura K, Shibata M, Ohura N, Fukuda T, Sato T, Sekine K, Kato S, Isshiki M, Fujita T, Kobayashi M, Kawamura K, Masuda H, Kamiya A & Ando J (2006). Impaired flow-dependent control of vascular tone and remodeling in P24-deficient mice. *Nat Med* **12**, 133–137.

Acknowledgements

We thank Dr Greg Fitz for his review of the manuscript and Dr Peter Igarashi for technical assistance with cilia staining. This study was supported by the Cystic Fibrosis Foundation (FERANC08G0), the Children's Medical Center Foundation, and the National Institute of Diabetes, Digestive and Kidney Diseases (NIDDK) of the National Institute of Health grant RO1 DK078587 (A.P.F.), and the UT Southwestern O'Brien Kidney Research Core Center (NIH P30DK079328).

Supplemental material

Online supplemental material for this paper can be accessed at:
http://jp.physoc.org/cgi/content/full/jphysiol.2008.153015/DC1
and
http://www.blackwell-synergy.com/doi/suppl/10.1113/jphysiol.2008.153015